

Seismic, Magnetic, and Geotechnical
Properties of a Landslide and
Clinker Deposits, Powder River
Basin, Wyoming and Montana

By Carter H. Miller

ARTHUR LAKES LIBRARY
COLORADO SCHOOL of MINES
GOLDEN, COLORADO 80401
CLOSED RESERVE

ProQuest Number: 11016554

All rights reserved

INFORMATION TO ALL USERS

The quality of this reproduction is dependent upon the quality of the copy submitted.

In the unlikely event that the author did not send a complete manuscript and there are missing pages, these will be noted. Also, if material had to be removed, a note will indicate the deletion.



ProQuest 11016554

Published by ProQuest LLC (2019). Copyright of the Dissertation is held by the Author.

All rights reserved.

This work is protected against unauthorized copying under Title 17, United States Code
Microform Edition © ProQuest LLC.

ProQuest LLC.
789 East Eisenhower Parkway
P.O. Box 1346
Ann Arbor, MI 48106 – 1346

A Thesis submitted to the Faculty and the Board of Trustees of the Colorado School of Mines in partial fulfillment of the requirements for the degree of Master of Engineering (Geophysical Engineering).

Signed: Carter H. Miller
Carter H. Miller

Golden, Colorado

Date: 3 - 30, 1979

Approved: PR Romig
Phillip R. Romig
Thesis Advisor

George V. Keller
George V. Keller
Department Head

Golden, Colorado

Date: 3 - 30, 1979

CONTENTS

	Page
Illustrations-----	iv
Tables-----	vi
Abstract-----	viii
Acknowledgments-----	x
Introduction-----	1
Preliminary discussion of seismic properties of clastic and clinker rocks-----	4
Calculator programs-----	13
Landslides-----	13
General geology-----	13
Springer Ranch landslide-----	15
Seismic investigations in the field surveys-----	17
Low-velocity layer-----	18
Thickness and configuration of the low-velocity layer-----	21
Correlation of the low-velocity layer with weathering and ground water-----	21
Shear waves, shear strength, and elastic moduli-----	23
Landslide model-----	26
Summary and conclusions-----	27
Clinker Deposits-----	30
Geology-----	30
Mode of ignition-----	30
Formation of clinkers-----	30

	Page
Clinker Deposits--continued	
Geotechnical properties-----	32
Temperature-dependent properties-----	33
Density, porosity, and fracture intensity-----	36
Hardness-----	37
Drillability-----	37
Geophysical properties, clinker study site, Gillette, Wyo.--	39
Magnetic properties-----	39
Magnetic survey-----	41
Measurement of hand samples compared to the	
results of laboratory and field surveys-----	45
Seismic properties-----	45
Laboratory measurements compared to field	
measurements-----	49
Summary and conclusions-----	49
References-----	53
Appendix I-----	57

ILLUSTRATIONS

	Page
Figure 1. Index map of the Powder River Basin, Wyoming and Montana, showing the sites of the Springer Ranch landslide, Gillette clinker study, and seven additional seismic lines (X SL-1)-----	2
2. Compressional-wave velocity distribution of the low-velocity layer (V_{p1}) and the underlying "layer" (V_{p2}) at the S-2 core hole, Sheridan, Wyo. <u>A</u> , Seismic velocity curves from ground-surface data. <u>B</u> , Lithology and least-squared seismic velocity from drill hole data-----	7
3. Compressional-wave velocity distribution of the low-velocity layer (V_{p1}) and the underlying "layer" (V_{p2}) at the B-1 core hole, Buffalo, Wyo. <u>A</u> , Seismic velocity curves from ground-surface data. <u>B</u> , Lithology and least-squared seismic velocity from drill hole data-----	8
4. Compressional-wave velocities and estimated economical dozing, ripping, and blasting capabilities of various rock types (nonweathered, --- weathered). Data from surface measurements in the Powder River Basin, Wyoming, from literature, and from estimates-----	10
5. A semiquantitative relationship of the texture and lithology of rocks and soils to V_p/V_s ratio and V_p magnitude (after Darracott, 1976)-----	12

	Page
Figure 6. The Springer Ranch landslide, showing topography, geologic structure, and location of seismic lines and drill holes-----	16
7. Velocity layering in the Springer Ranch landslide. <u>A</u> , Time-distance curves and geologic interpre- tations along seismic lines 1 and 2 (fig. 5) and <u>A-A'</u> . <u>B</u> , Isopach contours of the low-velocity layer determined by seismic refraction methods. <u>C</u> , Cross sections (<u>B-B'</u> , fig. 5) of velocity layering in the Springer Ranch landslide-----	19
8. Seismic properties of the low- and high-velocity layers of the Springer Ranch landslide. <u>A</u> , Shear- wave velocity as a function of approximate shear strength at failure (Imai and Yoshimura, 1975; Terzaghi and Peck, 1967). <u>B</u> , Seismic velocities, densities, elastic moduli, Poisson's ratio, and shear strength at failure-----	25
9. Clinker study area (fig. 1) showing sites of geo- technical, magnetic, and seismic investigations of clinkers (stippled) near Gillette, Wyo., along survey lines <u>A-A'</u> and <u>B-B'</u> -----	34
10. Some properties of clinkers as a function of temperature-----	35

Figure 11. Coefficient of rock strength of clinkers tested by the USGS (open) and compared to those rock types tested by Tandanand and Unger (1975) (darkened)-----	38
12. Representative net magnetism of various rock types (D. E. Watson, unpub. data, November 1976)---	40
13. Magnetic field intensity (normalized to 58,595.0 gammas) and seismic surveys along <u>B-B'</u> (fig. 9)-----	42
14. Geotechnical, magnetic, and seismic surveys along <u>A-A'</u> (fig. 9)-----	44
15. Field and (hand samples (open)) and laboratory (core (dark)) measurements of remanent magnetism and Earth's total magnetic field intensity run on clinkers along <u>A-A'</u> (fig. 9, 14)-----	46
16. In situ (open) and laboratory (dark) measurements of compressional- (V_p) and shear- (V_s) wave velocities, the dynamic-elastic moduli (E = Young's; G = shear; B = bulk), and Poissons's ratio (σ) run on clinkers along <u>A-A'</u> (figs. 9, 14)-----	50

TABLE

	Page
Table 1. Compressional- (V_{p1}) and shear- (V_s) wave velocities of the low- (V_1) and high- (V_2) velocity layers and approximate thickness of the V_1 layer for clastic and clinker rocks, Powder River Basin, Wyoming, and some compressional velocities for clastic rocks from the Soviet Union-----	6

Seismic, Magnetic, and Geotechnical Properties
of a Landslide and Clinker Deposits, Powder River
Basin, Wyoming and Montana

By Carter H. Miller

ABSTRACT

Exploitation of vast coal and other resources in the Powder River Basin has caused recent, rapid increases in population and in commercial and residential development and has prompted land utilization studies. This thesis was funded by the U.S. Geological Survey and it reports two aspects of land utilization: (1) the seismic and geotechnical properties of a landslide and (2) the seismic, magnetic, and geotechnical properties of clinker deposits.

(1) The landslide seismic survey revealed two layers in the slide area. The upper (low-velocity) layer is a relatively weak mantle of colluvium and unconsolidated and weathered bedrock that ranges in thickness from 3.0 to 7.5 m and has an average seismic velocity of about 390 m/s. It overlies high-velocity, relatively strong sedimentary bedrock that has velocities greater than about 1330 m/s. The low-velocity layer is also present at the other eight seismic refraction sites in the basin; a similar layer has also been reported in the Soviet Union in a landslide area over similar bedrock.

The buried contact of the low- and high-velocity layers is relatively smooth and is nearly parallel with the restored topographic surface. There is no indication that any of the high-velocity layer (bedrock) has been displaced or removed.

The seismic data also show that the shear modulus of the low-velocity layer is only about one-tenth that of the high-velocity layer and the shear strength (at failure) is only about one-thirtieth. Much of the slide failure is clearly in the shear mode, and failure is, therefore, concluded to be confined to the low-velocity layer. The major immediate factor contributing to landslide failure is apparently the addition of moisture to the low-velocity layer.

The study implies that the low-velocity layer can be defined over some of the basin by seismic surveys and that they can help predict or delineate potential slides. Preventative actions that could then be taken include avoidance, dewatering, prevention of saturation, buttressing the toe, and unloading the head. The low-velocity layer is usually less than about 5 m thick and may be excavated by dozing, whereas the bedrock must be blasted. Thus, it would seem economically feasible to underpin a structure to nonweathered bedrock or, perhaps, to remove the low-velocity layer prior to construction.

(2) Many coal beds in the Powder River Basin have burned along their outcrops, and the resulting intense heat has baked and fused the overlying clastic (sedimentary) rocks into clinkers. The clinkers are very magnetic and a buried edge of a single layer of burn can easily be located by magnetic prospecting methods. Location of the edge is very important in estimating unburned coal deposits, locating clinker quarries, and planning drilling of seismic reflection lines.

The clinkers are very porous and highly fractured, and seismic and geotechnical tests show that they have relatively low strength and competency. Many of the laboratory tests, however, are inherently biased because the clinkers are so highly fractured that only competent

samples are selected. The laboratory tests, for example, show that clinkers must be loosened by heavy ripping tractors or blasting, whereas the field data and practical experience indicate that clinkers may be mined with light equipment.

Heavy structures such as coal silos and bridge abutments may have to be sited on clinkers. However, differential settlement may occur, with failure in the shear mode, because chimneys of relatively greater strength occur among the weaker clinkers. Preliminary data indicate that the chimneys may be located by magnetic or possibly seismic surveys. Special foundation-preparation techniques could be used or, perhaps, the chimneys could be avoided altogether at a construction site.

ACKNOWLEDGMENTS

This report was prepared as a graduate thesis in partial fulfillment of the requirements for a Master of Engineering degree from the Colorado School of Mines. It is based on research conducted under the Energy Lands Program of the U.S. Geological Survey.

Technical assistance and guidance from planning through completion stage were provided by members of the Colorado School of Mines: Phillip R. Romig (Chairman), Keith A. Turner, and George R. Pickett.

U.S. Geological Survey personnel who supported the studies include Richard A. Farrow, Abelardo L. Ramirez, and Thomas F. Bullard, who participated in the seismic surveys and data reductions, and Stanley L. Obernyer, who participated in the seismic surveys. Kent A. Hewitt, Jackson K. Odum, and Philip S. Powers did the drilling,

and they and David M. Worley did most of the core testing.
Alan F. Chleborad, Richard A. Farrow, William P. Hasbrouck,
Frank W. Osterwald, and Donald E. Watson provided technical assistance.

We thank C. A. "Dick" Springer for permitting access to the
landslide on his property and for his enthusiastic support.

INTRODUCTION

Exploitation of vast coal and other resources in the Powder River Basin, Wyoming and Montana (fig. 1), has caused rapid increase in population and in commercial and residential development in the basin since the mid-1970's. This rapid expansion is expected to continue, and the results of engineering geology studies by the U.S. Geological Survey will help ensure intelligent land utilization during this sudden expansion. This report concerns two aspects of land utilization: (1) the seismic and geotechnical properties of a landslide and (2) the seismic, magnetic, and geotechnical properties of a clinker deposit. The objectives of the study are to investigate the character and properties of the landslide and the clinker deposits so that other landslide hazards can be dealt with and other clinker deposits can be delineated and exploited by using the principles learned in this study.

The studies were done in the central part of the basin, where the bedrock may be either soft, interbedded sandstone, shale, clay, and coal of the Tertiary Wasatch or Fort Union Formation or clinker deposits. The soft sedimentary rocks of the Wasatch and Fort Union Formation are called clastic rocks in this report, and the term "clinker deposits" is meant to include all baked and fused clastic rocks as well as any coke and ash residue from the burned coal (Bauer, 1972). Both the clastic rocks and clinkers may be overlain by alluvium or colluvium, or by residual or eolian deposits, but the clinkers may be included in clastic rocks.

Landsliding is one of several geologic hazards to development in the Powder River Basin. These landslides presently cause damage mainly to highways and agricultural land, but future construction may be

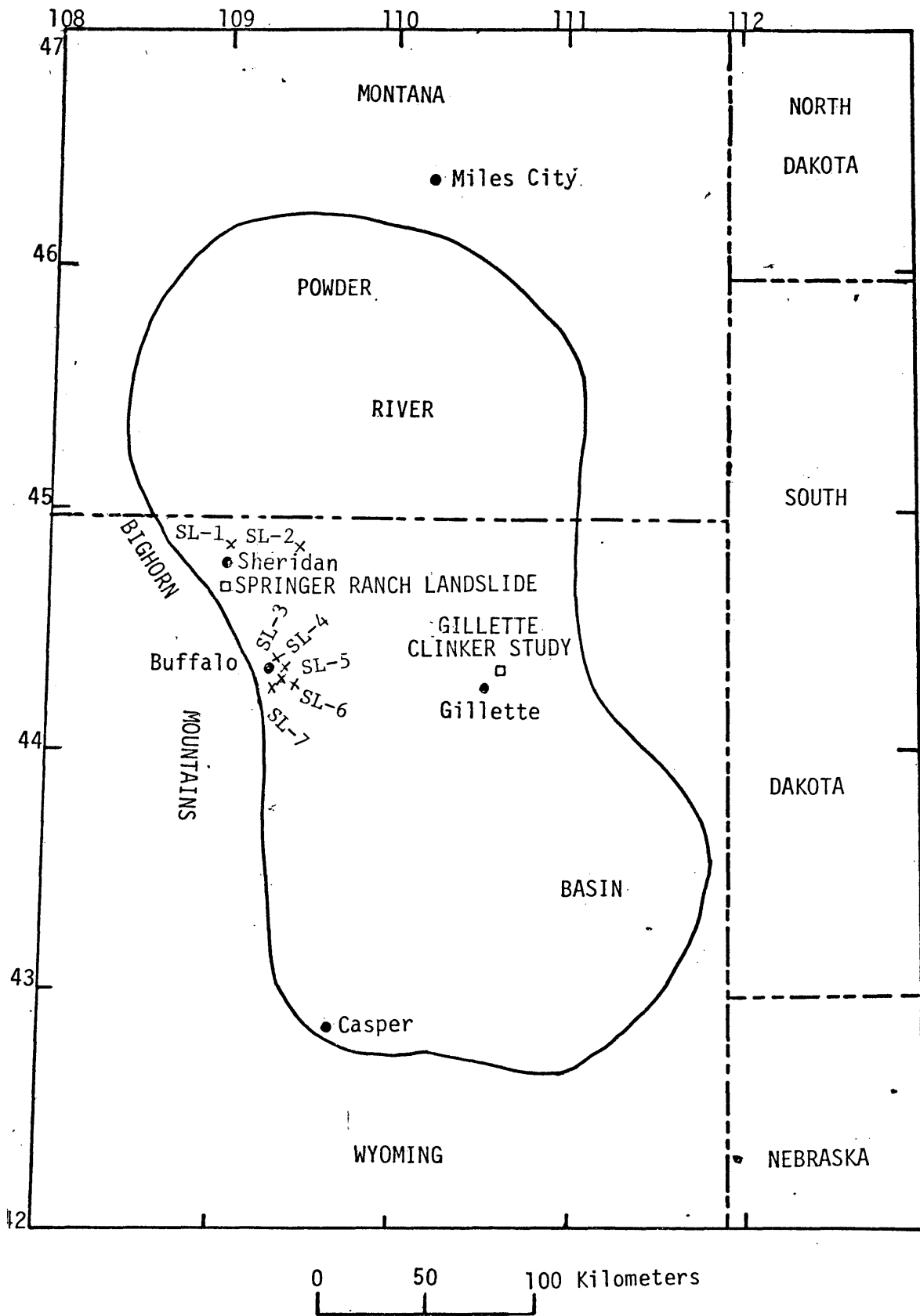


Figure 1.--Index map of the Powder River Basin, Wyoming and Montana, showing the sites of the Springer Ranch landslide, Gillette clinker study, and seven additional seismic lines (X SL-1).

inadvertently or necessarily sited on a potential slide or in its path. The present report is a study of one such landslide, here called the Springer Ranch landslide (fig. 1), by seismic-refraction techniques that use both compressional waves and shear-waves.

There are striking and predictable similarities between the seismic properties at the Springer Ranch landslide and those at other seismic-measurement sites over soft, clastic bedrock. These sites include several in the Powder River Basin and one in the Soviet Union, and they will be discussed later in this report. These similarities imply that seismic and engineering geologic surveys can be applied in the delineation of unstable slopes in the Powder River Basin. If unstable slopes in the basin can be delineated, then corrective actions such as avoidance, dewatering, buttressing the toes, unloading the head, or removal of the potential slide material can be taken.

Many coal beds in the Powder River Basin have burned along their outcrops, and the resulting intense heat has baked and fused the overlying clastic rocks into clinkers. The extent that the coal has burned into the subsurface is not necessarily apparent from the surface, but magnetic methods can delineate the edge of a single layer of buried clinkers. Location of the edge is very important in estimating (nonburned) coal deposits, in locating clinker quarries, and in planning drilling or seismic reflection lines for projects, whose success may depend on the absence of clinkers. Much of the new construction in the basin may have to be sited near economic coal deposits, but not on them. Hence, clinker deposits may be the logical sites for some future construction, and knowledge of the extent of buried clinkers would, therefore, be necessary.

The clinkers are very porous and highly fractured, and their relatively low strength belies their erosion-resistant qualities. In much of the basin, however, the clinkers are the only hard material available for building highways and railroads and for use as lightweight aggregate.

Heavy structures such as coal silos and bridge abutments may have to be sited on clinkers. Differential settlement with failure in the shear mode may occur, however, because chimneys of relatively greater strength occur among the weaker clinkers. Special foundation-preparation techniques may have to be used or, perhaps, chimneys can be located by geophysical methods and avoided at the building sites.

Preliminary discussion of seismic properties
of clastic and clinker rocks

Seismic techniques and their results are the major part of both the landslide and clinker-deposit studies. Therefore, the subjects common to both places will be given a preparatory discussion here.

Seismic refraction lines were run at the Springer Ranch landslide, at the Gillette clinker-study site, and at seven additional sites shown in figure 1 (R. A. Farrow, C. H. Miller, and A. L. Ramirez, written commun., April 1977). All of these seismic lines were run over either clastic rocks or clinkers, and the resulting compressional- and shear-wave velocities are summarized in table 1. The compressional-wave data indicate that:

1. A low-velocity layer (V_{p1}) overlies a high-velocity layer (V_{p2}) at all of the sites in the Powder River Basin. The velocities of the low-velocity layer are essentially the same for both clinkers

and clastic rocks: they range from 350 to 470 m/s and average 390 m/s.

2. The high-velocity V_{p2} layer of clinkers is poorly developed, but where it is present its compressional-wave velocities are considerably less than those for clastic rocks. The velocities for this V_{p2} layer in the clinkers range from 490 to 760 m/s and average 630 m/s, while those for clastic rocks range from 710 to 1950 m/s and average 1330 m/s.

Figures 2 and 3 show the compressional-wave velocity distribution of the low-velocity layer (V_{p1}) and the underlying "layer" (V_{p2}) at core holes (R. A. Farrow, written commun., 1978) in Sheridan (S-2) and Buffalo (B-1), Wyoming (R. A. Farrow, written commun., 1976). Sonic logs were run in the core holes to within about 12 m of the ground surface by Birdwell, Inc., Tulsa, Okla., and seismic refraction lines were run at ground surface by the author and R. A. Farrow (U.S. Geological Survey).

Although the S-2 hole is cored into the Fort Union Formation and the B-1 hole is in the Wasatch Formation, and the two holes are about 60 km apart, the compressional-wave velocities of both the low-velocity layer and the underlying high-velocity V_{p2} "layer" are quite similar. The inhole velocities of both holes were all recorded from the V_2 "layer," and the best least-square fit was obtained for both linear and logarithmic functions of depth for each hole. The best fit for the velocities of each hole is probably the logarithmic curve, but the

Table 1.--Compressional- (V_{p1}) and shear- (V_s) wave velocities of the low- (V_1) and high- (v_2) layers and approximate thickness of the V_1 layer for clastic and clinker rocks, Powder River Basin, Wyoming, and some compressional velocities for clastic rocks from the Soviet Union

Seismic Line	Velocity (m/s)				Approximate Thickness V_1 layer (m)	Lithology of V_2 layer
	Compressional wave		Shear wave			
	V_{p1} layer	V_{p2} layer	V_{s1} layer	V_{s2} layer		
1-----	350	1710	---	---	5	Clastic rocks.
3-----	420	1950	---	---	3	Do.
7-----	350	1210	---	---	3	Do.
Springer Ranch Landslide.	400	1470	127	530	4-8	Do.
4-----	440	910	---	---	8	Clastic rocks (coal/clinker?).
Gillette Clinker- Study Area.	370	710	---	---	4	Clastic rocks (coal?).
	350	710	230 ¹	---	>12	Clinkers.
2-----	350	760	---	---	4	Do.
5-----	440	610	---	---	2	Do.
6-----	470	650	---	---	6	Do.
Sochi, Black Sea Coast, Caucasas Mountains (Bogoslovsky and Ogilvy, 1977).	340-360	1360-1400	---	---	3-17	Fractured and "nonweathered" argillite.

¹ One shear-wave velocity line was run where there was no velocity layering.

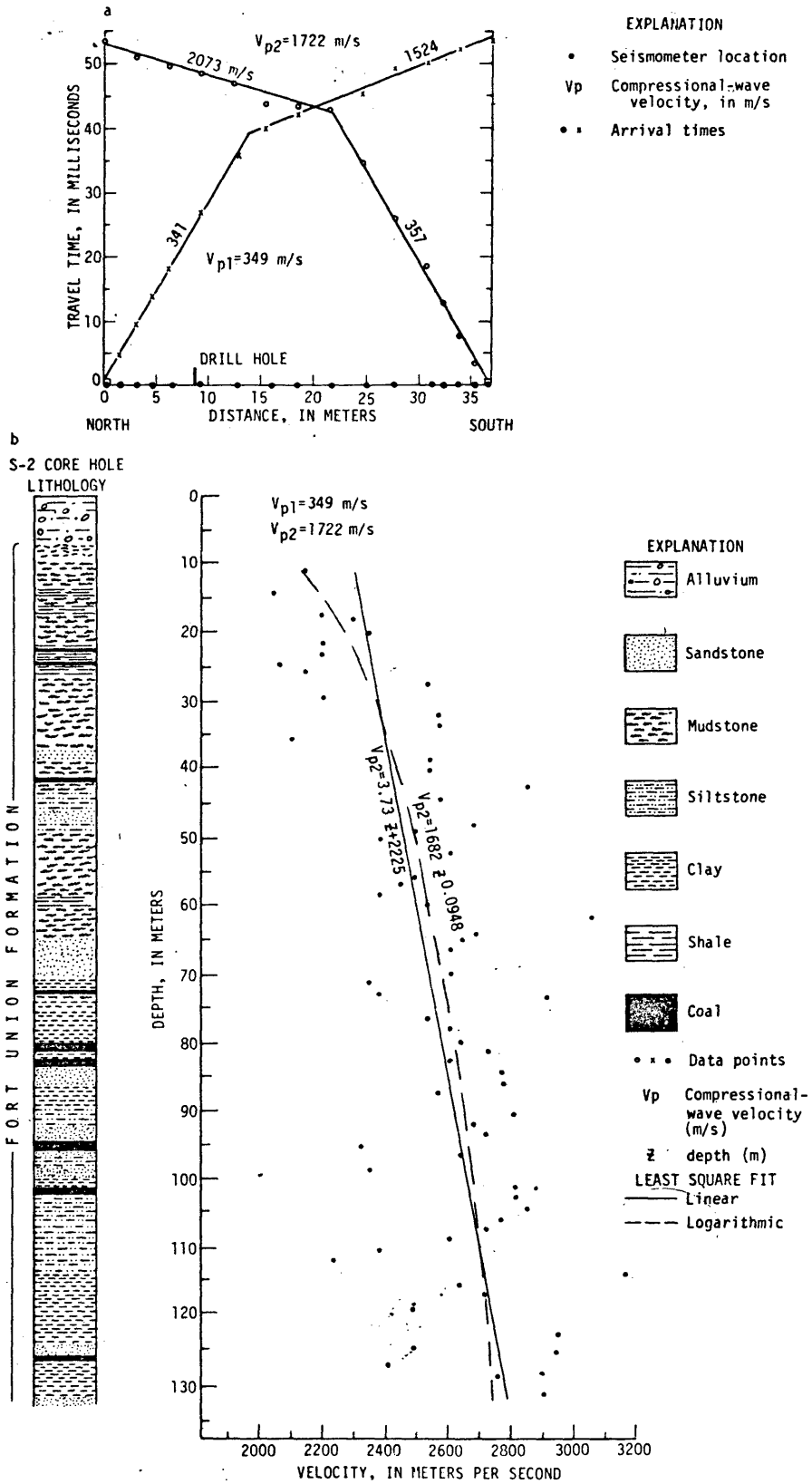
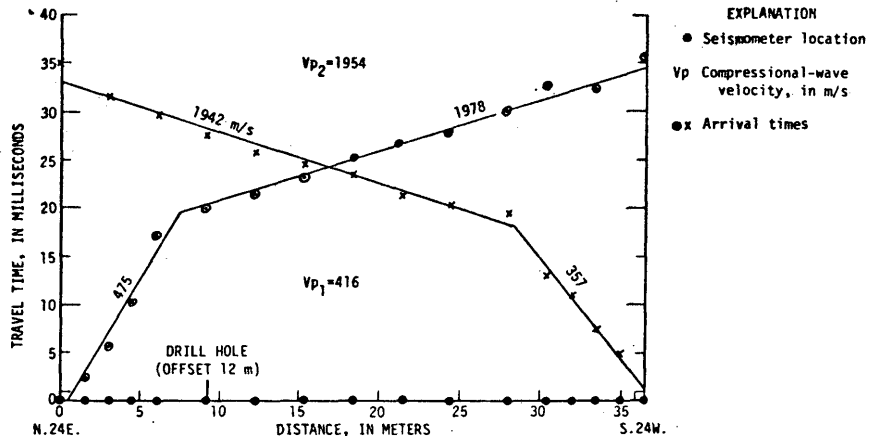


Figure 2-- Compressional-wave velocity distribution of the low-velocity layer (V_{p1}) and the underlying "layer" (V_{p2}) of the S-2 core hole Sheridan, Wyoming. a, Seismic velocity curves from ground. b, Lithology and least-squared seismic velocity from drill hole data.



**LITHOLOGY
B-1 CORE HOLE**

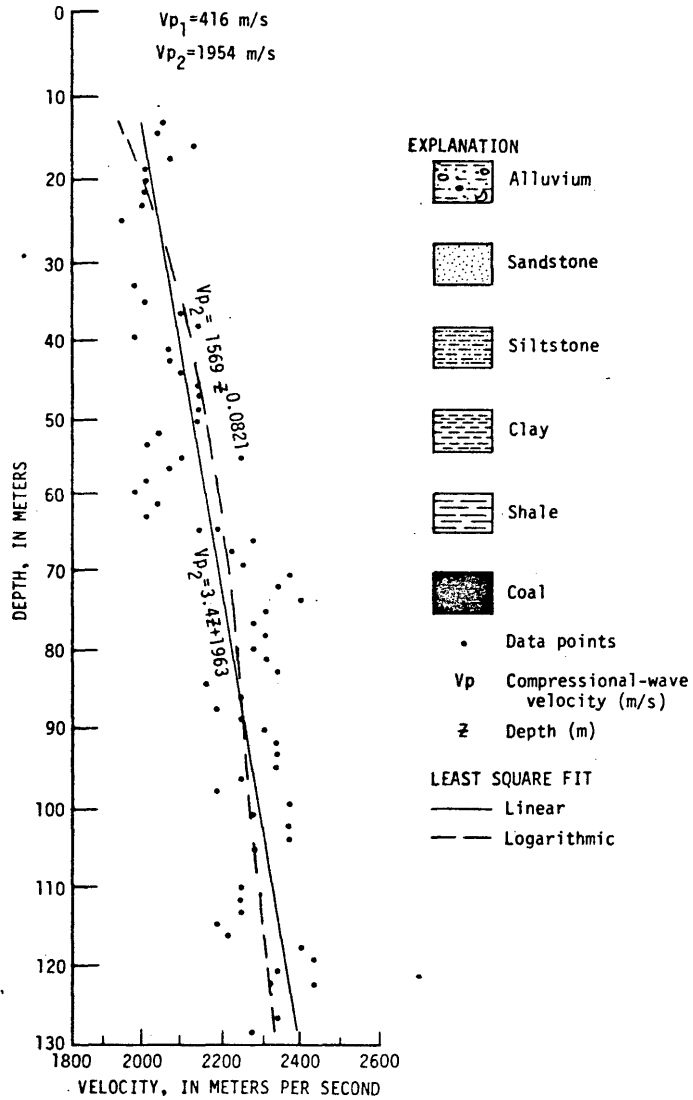


FIGURE 3.--Velocity distribution of the low-velocity layer (V_{p1}) and the underlying "layer" (V_{p2}) at the B-1 core hole, Buffalo Wyoming. a, Seismic velocity curves from ground-surface data. b, Lithology and least-squared seismic velocity from drill hole data.

velocity gradients of the linear fits are more easily compared: these are 3.7 m/s/m of depth in the S-2 hole and 3.4 m/s/m in the B-1 hole.

The average seismic velocity for a 5-m-thick low-velocity layer at the S-2 hole is 349 m/s, while that for a 2.4-m thickness at the B-1 hole is 416 m/s. The V_{p1} - V_{p2} interface at either core hole does not particularly correlate with the alluvium-clastic rock interface. Both core holes are collared on flood plains, however, and each velocity interface is apparently at the surface of a well-developed ground-water table in unconsolidated alluvium. The least-squares inhole velocity is 1960 m/s at the top of the V_{p2} "layer" in the S-2 hole, compared to 1722 m/s at the same depth by the surface-refraction method. The least-squares velocity in the V_{p2} "layer" for the B-1 hole is 1686 m/s, compared to 1954 m/s by the surface refraction method.

There is an empirical relation between the compressional-wave velocity and the quality or relative strength of most rocks and soils; the higher the compressional-wave velocity of the rocks and soil, the higher is their relative strength (Darracott, 1976). Figure 4 compares the compressional-wave velocities of clastic rocks and clinkers from near-surface measurements in the Powder River Basin with compressional-wave velocities of other rocks. All of the clastic rocks of the low-velocity layer have compressional-wave velocities and velocity ranges considerably lower than those of the other nonweathered rocks and are, therefore, apparently of relatively low strength.

Economical dozing, ripping, and blasting capabilities (Caterpillar Tractor Co., 1972) of rocks are also related to seismic compressional-wave velocities in figure 4. The graph indicates that all of the clinkers as well as the clastic rocks of the low-velocity layer may be

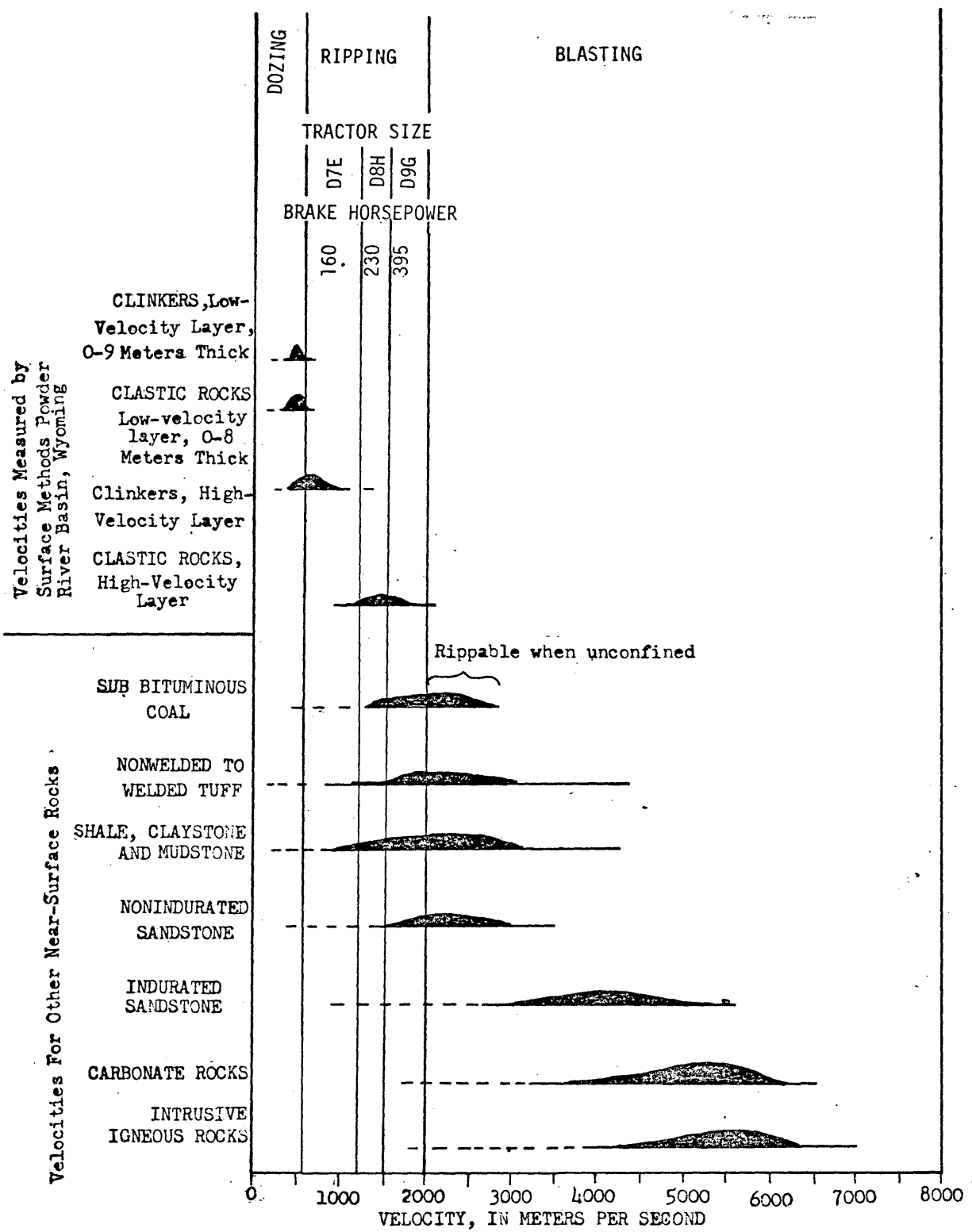


Figure 4- Compressional-wave velocities and estimated economical dozing, ripping, and blasting capabilities of various rock types (— nonweathered, --- weathered). Data from surface measurements in the Powder River Basin, Wyoming, from literature, and from estimates.

dozed. The clastic rocks of the high-velocity layer may be ripped with a heavy tractor, but not dozed, and blasting is unnecessary for shallow excavations in this layer.

Degree of saturation and amount and size of voids are important parameters that affect rock and soil quality and relative strength, but which may not necessarily be accurately indicated by compressional-wave velocity. Shear waves, however, cannot be transmitted by either air or water in voids, and shear-wave velocity is, therefore, an indicator of the presence of air or water.

Much of the slope failure at the Springer Ranch landslide was clearly in the shear mode, and any differential settlement of a heavy structure sited on clinker deposits is also expected to promote failure in the shear mode. Shear strength of rocks and soil at failure varies with shear-wave velocity and, hence, relative shear strengths at the landslide and clinker-deposit site can be derived from shear-wave velocity measurements. The velocities of table 1, therefore, indicate that the shear strength (at failure) of the V_2 layer associated with clastic bedrock is much greater than that of either the V_1 layer of clastic rocks or of any layer of clinkers and that the shear strength of any of the clinkers is greater than that of the V_1 layer of clastic rocks. This concept is applied to the Springer Ranch landslide and the Gillette clinker deposits.

Figure 5 shows a semiquantitative relationship of rock and soil texture and lithology to V_p/V_s ratio and V_p magnitude for a given layer (Darracott, 1976). The V_p velocities and V_p/V_s ratios for both layers of clinkers and clastic rocks (table 1) are plotted on figure 5. The plot indicates that the ratio is about 3.2 for the clastic rocks of the

EXPLANATION

V_{p1} Compressional wave velocity in meters per second (m/s), uppermost layer.

V_{p2} Compressional wave velocity in meters per second (m/s), underlying layer.

V_s Shear-wave velocity

○ clastic rocks
 X clinkers

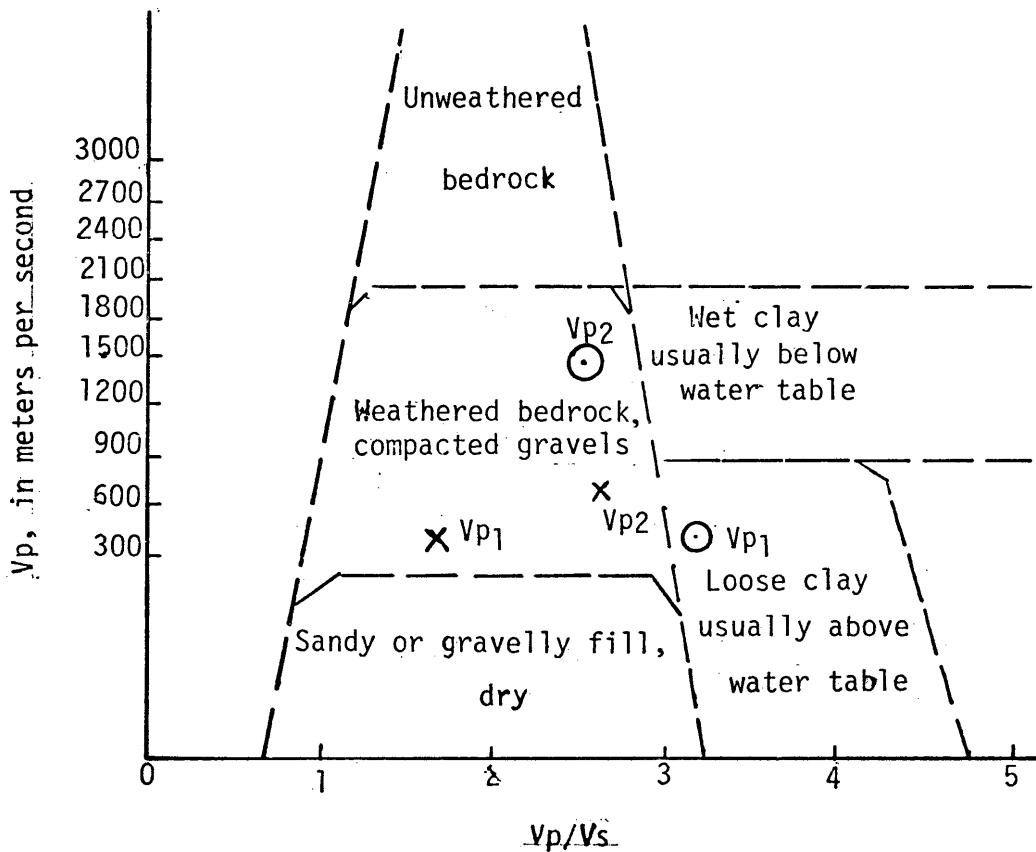


Figure 5- A semiquantitative relationship of the texture and lithology of rocks and soils to V_p/V_s ratio and V_p magnitude (after Darracott, 1976).

V_1 layer in the Powder River Basin and 2.8 for the V_2 layer, while the ratio is 1.5 for the V_1 layer and 2.1 for the V_2 layer of the clinker deposits at the Gillette, Wyo., site. The plot (fig. 5) also shows that the V_2 layer for clastic rocks has higher relative strength than either the V_2 layer for clinkers or V_1 layers for clinkers and clastic rocks. Although the compressional-wave velocities for the V_1 layer of clastic rocks and clinkers are similar, the V_1 layer for clastic rocks is wetter, more clayey, and finer grained than is the V_1 layer for clinkers.

Calculator programs

Hewlett Packard 65 calculator¹ programs were written for much of the data reduction. These programs include: (1) depth and configuration of a buried refraction velocity layer, (2) elastic constants, and (3) stadia-alidade traverse reductions, all by Miller and Bullard (1978a, b, c). They comprise Appendix I; an abstract description, program steps, and instructions with examples are included.

LANDSLIDES

General geology

Preliminary landslide investigations in the western Powder River Basin were made by Chleborad, Nichols, and Ebaugh (1976) and Ebaugh (1976, 1977) as part of continuing engineering geology studies. These investigations have included much of the northwestern part of the basin, but emphasis was placed on an area of 300 km² southeast, south, and west

¹Use of a brand name in this report is for descriptive purposes only and does not constitute endorsement by the U.S. Geological Survey.

of the city of Sheridan, Wyo. (fig. 1), where extensive slope failures have occurred.

Bedrock in this area of greatest slope failure comprises shales, fine-grained sandstones, and coals of the Fort Union Formation and overlying Wasatch Formation (Mapel, 1959). Both of these Tertiary formations dip slightly to the east away from the Bighorn Mountains and toward the axis of the Powder River Basin (fig. 1). Ground-water resources have been reported by Lowry and Cummings (1966).

A mantle of unconsolidated or weathered bedrock, clay, silt, sand, gravel, boulders, and soil covers much of the bedrock in the study area. Terrace and pediment deposits of the area are as much as 14 m thick, and flood-plain deposits are as much as 30 m thick, but the thickness of colluvium seldom exceeds 3 m on the slopes (Mapel, 1959). Weak, weathered bedrock, however, locally underlies the colluvium.

Slopes that are cut in nonweathered bedrock for highways and coal strip mines in the basin do not readily fail. The strip-mine walls are nearly vertical and as much as 30 m high, but they rarely fail within a few months' time, and their lifespan may be years. Most highway cuts are of low angle slope, and the lifetime of these bedrock cuts may be decades of time. Slope failures, except for large slides that were promoted by highway construction and by streams that undercut the toes of potentially unstable slopes, seem to be confined to the mantle of alluvium, colluvium, and unconsolidated or weathered bedrock. Nonweathered bedrock apparently is not included in the relatively small landslides.

In a detailed study of the factors that promote landsliding in the Big Horn quadrangle, which includes the Springer Ranch landslide, Ebaugh

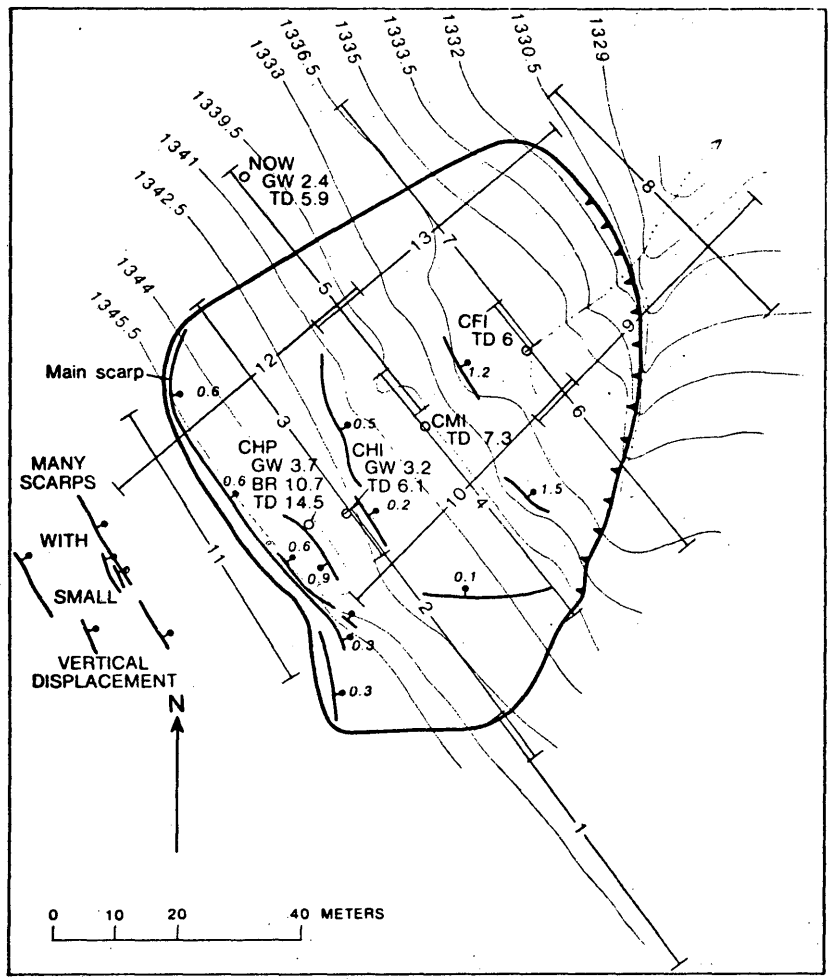
(1977) found that most slides occur on slopes facing in the direction of bedrock dip. He concluded that, on these slopes, artesian pore-water pressures can develop where clayey colluvium seals an outcropping bedrock aquifer. Through the principle of effective stress, these high pore pressures act to reduce effective normal stresses and thus the material's shear strength. Ebaugh believes that failures tend to occur at the base of the colluvial layer.

Springer Ranch landslide

The Springer Ranch landslide is about 14 km south-southeast of Sheridan, Wyo. (fig. 1). It was selected for special study as representative of other slides in the area because of its geometry, slope, and orientation. The author did detailed seismic-refraction and elastic moduli investigations (C. H. Miller, A. L. Ramirez, and T. F. Bullard, oral commun., 1978), in conjunction with other members of the U.S. Geological Survey, who drilled the slide and installed piezometers and inclinometers in the drill holes. The drill holes were geologically logged, and static water levels and some physical properties of the mantle and underlying bedrock were measured.

Figure 6 shows the topography and geologic structure of the Springer Ranch landslide. The slide is on a northeast-facing slope. The limits of the slide are defined by either fresh fractures or by sudden changes in slope, where healed fractures are evident. It is about 75 m long by 75 m wide, and has moved down a gradient of about 5:1 (11°). Bedrock dip in this area is about 1° NE.

Tensional and shear failure, with resulting slumps and open fractures, occurs at the head of the slide. The conspicuous main scarp at the head of the slide has at least 3 or 4 m of horizontal



- EXPLANATION**
- Perimeter of landslide--Showing overthrusting at part of limit. Teeth are on upper plate
 - Recent scarp--Showing vertical displacement, in meters. Bar and ball on downthrown side. Dashed where inferred
 - Drill hole--Showing designation (CHP); depth to ground water (GW); depth to unweathered bedrock (BR); and total depth (TD), in meters
 - 1329— Contour interval 1.5 meters--Mapped by plane-table method; datum estimated from U. S. Geological Survey 7 1/2 minute Bighorn quadrangle
 - 5— Seismic line and number

Figure 6--The Springer Ranch landslide, showing topography, geologic structure, and location of seismic lines and drill holes.

displacement and 0.6 m of vertical displacement. Many small scarps are evident uphill from the main scarp.

Shear failure, with accompanying earthflow, is apparent in the toe of the slide. Net movement to the northeast was accompanied by an "overthrust" bulge and apparent relocation of the course of a small intermittent stream. The horizontal distance that the bulge has "overthrust" onto the old land surface is unknown.

Five holes (fig. 6) were drilled and studied in the slide area. Lithologies included clay, shale, and fine-grained, unconsolidated sandstone (Ebaugh, 1977). Both fresh unweathered bedrock and the overlying weathered zone were defined on the basis of the state of relative oxidation: dark-gray to blue-gray fresh bedrock was considered to be in the reduced state; the oxidized weathered zone above was brown, orange, and yellow, in varying proportions, and the contact between the weathered zone and the fresh unweathered bedrock is gradational. Drill hole CHP penetrated bedrock at 10.7 m, but bedrock was not found in the other four holes, whose depths ranged from 5.9 to 7.3 m.

Ground-water levels were also measured in three of the five holes. These levels were probably influenced by drilling fluids, and the true ground-water levels probably fluctuate seasonally.

Seismic investigations in the field surveys

Seismic investigations of the Springer Ranch landslide were of two types: a refraction (compressional-wave) survey to determine the thickness and configuration of the slide, and a shear-wave survey to determine the shear modulus and approximate shear strength of both the landslide and the underlying material that had not failed.

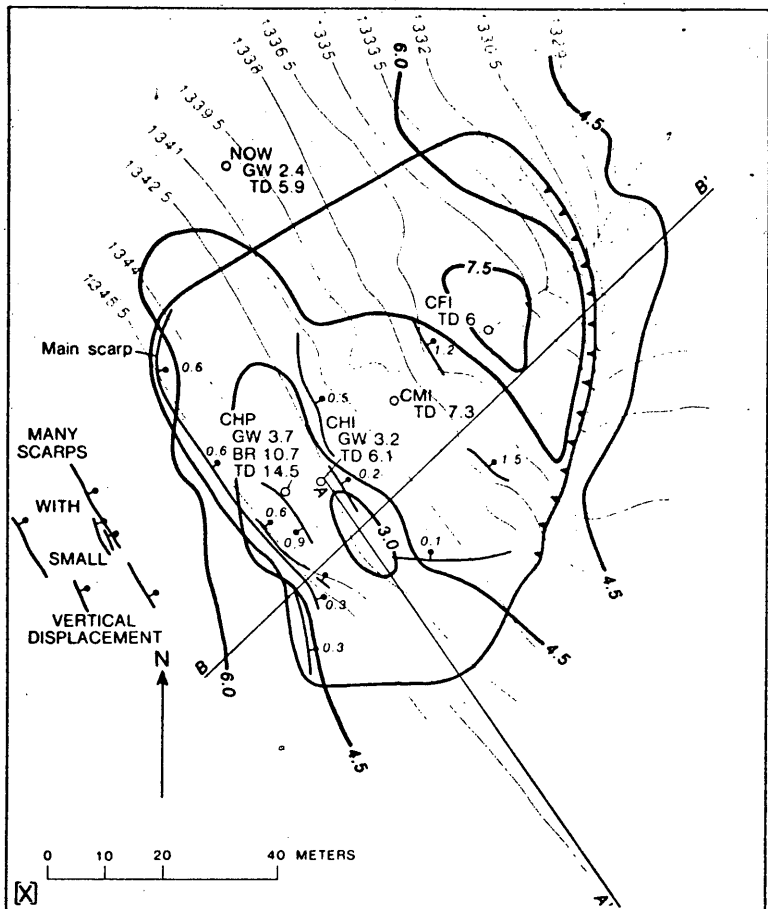
Thirteen seismic-refraction lines (fig. 6) were run, and one shear-wave line reoccupied the position of refraction line 2. The seismic lines were oriented mainly either parallel or perpendicular to the hillside, and lines were extended to the perimeter of the landslide. Line 1 was located completely off the landslide to provide seismic data that could be compared with data from lines on the slide.

Twelve seismometers were emplaced along each line at 4.2-m intervals for both the refraction and shear-wave surveys. Each line was 50.3 m long, and where the lines were end to end they were overlapped 8.4 m to provide continuous information at depth. The shotpoints for the refraction lines were directly under the end seismometers and were in shotholes that were about 0.6 m deep. Charges in the shotholes were equivalent to about 150 g of 60 percent dynamite, and were detonated with electric caps. The energy source for the shear-wave line was also at the end seismometers of line 2. This source was a wooden plank weighted down and oriented perpendicular to the seismic line. Horizontally oriented geophones were planted for the shear-wave surveys, and the ends of the plank were struck with a sledge hammer. The directions of the blows were alternated for each seismogram, so that reversed particle motion could be observed on the seismogram.

Low-velocity layer

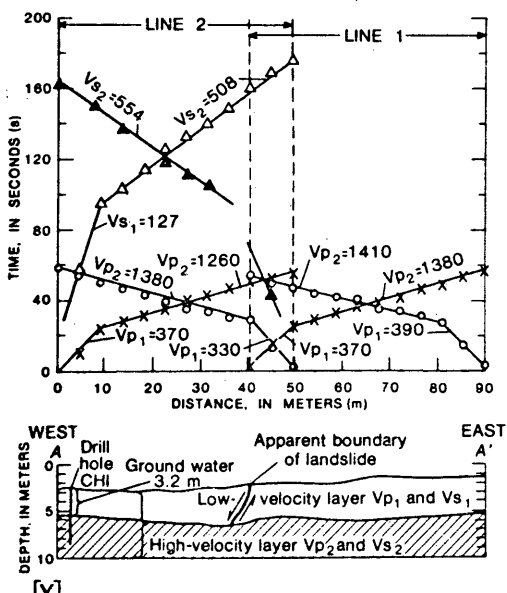
Figure 7A shows the time-distance curves for seismic lines 1 and 2. The methods of measurement along each line are the same, but line 1 is off the slide, whereas line 2 is on it.

Two velocity layers (table 1) are clearly defined by the time-distance curves of both lines 1 and 2: an upper low-velocity layer and an underlying high-velocity layer. These two velocity layers are also

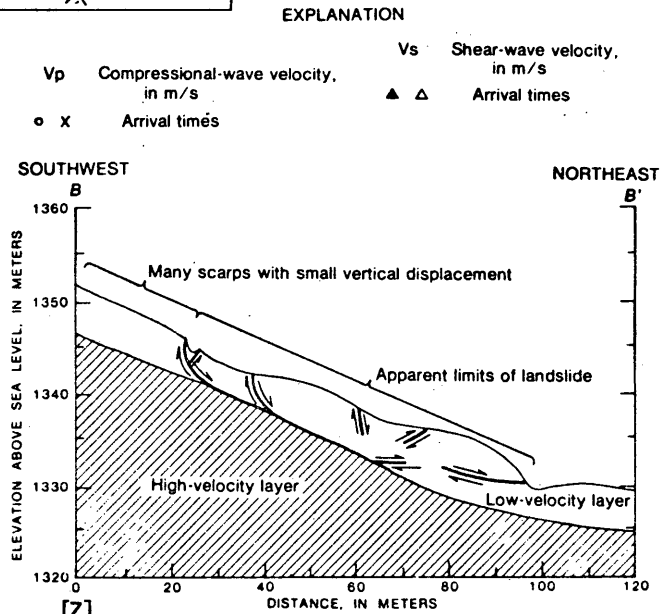


- EXPLANATION**
- Perimeter of landslide--Showing overthrusting at part of limit. Teeth are on upper plate
 - Recent scarp--Showing vertical displacement, in meters. Bar and ball on downthrown side. Dashed where inferred
 - Drill hole--Showing designation (CHP); depth to ground water (GW); depth to unweathered bedrock (BR); and total depth (TD), in meters
 - Contour interval 1.5 meters--Mapped by plane-table method; datum estimated from U. S. Geological Survey 7 1/2 minute Bighorn quadrangle
 - Isopach contour of the low-velocity layer--Contour interval is 1.5 meters

(b.) Isopach contours of the low-velocity layer determined by seismic refraction methods.



(a.) Time-distance curves and geologic interpretations along seismic lines 1 and 2 (fig. 5) and A-A'.



(c.) Cross section (B-B', fig. 6) of velocity layering in the Springer Ranch landslide.

Fig. 7-Velocity layering in the Springer Ranch landslide

defined by all the other seismic lines on the landslide. In addition, the other seismic lines that have been run in the northern part of the Powder River Basin and away from the Springer Ranch landslide (table 1) also define two velocity layers. The average velocity of the low-velocity layer along line 1, off the slide, is 380 m/s, while the average velocity of the 12 lines on the slide is 407 m/s. The average velocity of the seismic lines in other parts of the basin is 390 m/s. I conclude, therefore, that (1) there is no appreciable velocity contrast within the low-velocity layer between the Springer Ranch landslide and adjacent undisturbed ground, (2) the low-velocity layer includes the landslide at the Springer Ranch, but then buried main surfaces of rupture of the slide will not all necessarily coincide with the lower boundary of the low-velocity layer, and (3) the low-velocity layer extends into at least part of the Powder River Basin.

A landslide near the town of Sochi, on the Black Sea coast of the Caucasus Mountains, was studied by Bogoslovsky and Ogilvy (1977), who described it as "composed of loamy rocks underlain by a weathered crust of argillites." The loam and weathered argillite is underlain by fractured but nonweathered argillite. "Seismic measurements identified a single boundary that divides the landslide slope into two distinct masses of rock. The upper one (with $V = 340-360$ m/s) comprises the landslide body and the slip zones and the lower one (with $V = 1360-1400$ m/s) corresponds to the upper surface of the argillites."

These velocities of the Sochi landslide are compared with those measured in the Powder River Basin and the Springer Ranch landslide in table 1. Although the studies were done independently the velocity

measurements are very similar, which suggests that some seismic surveys over clastic rocks with V_1 and V_2 layers may be comparable.

Thickness and configuration of the
low-velocity layer

Thickness and configuration of the low-velocity layer at the Springer Ranch landslide were interpreted from the seismic-refraction data by the method of differences (Laby, 1931, p. 637-671, modified by J. C. Hollister, Colo. School of Mines, unpub. data, 1957; Redpath, 1973). The advantage of this method is that it accounts for variations in thickness of the low-velocity layer. The variations may be due to changes in the surface topography, in the topography of the buried contact between the low-velocity and high-velocity layers, or in both. The results of the interpretation of thickness and configuration of the low-velocity layer at the slide are summarized by the isopach map and by cross sections A-A' of figures 4 and 5 and B-B' of figure 7C.

Although the seismic lines were run over undulating topography, the contact between velocity layers does not undulate, and it is nearly parallel with the restored topographic surface. The thickness of the low-velocity layer is about 3.0 m at the head of the slide, but it is more than 7.5 m at the toe bulge, which supports the observation that the toe of the slide is overthrust on a relatively undisturbed, low-velocity layer. The thickness of the undisturbed low-velocity layer away from the slide ranges from about 4.5 to 6.0 m.

Correlation of the low-velocity layer
with weathering and ground water

Although the velocity curves (fig. 7A) clearly show two velocities whose layers contact at the depth shown by the isopach map (fig. 7B),

the refraction path is through subweathered bedrock and above unweathered bedrock. The unweathered bedrock, however, is defined by visual inspection of cores from only one drill hole, CHP. The seismic waves, nevertheless, travel through the subweathered zone about four times faster than through the low-velocity layer. The velocity of propagation of compressional waves depends upon the elastic moduli of the media, and the high-velocity layer is proportionately stronger than the low-velocity layer. Relatively strong bedrock, therefore, is here defined by the high-velocity layer, and the relatively weak mantle that overlies it is defined by the low-velocity layer. The mantle includes colluvium and unconsolidated and weathered bedrock, and the high-velocity layer apparently includes subweathered as well as weathered bedrock.

Figure 6 shows that three of the five drill holes penetrated static ground-water level. The levels, however, are dependent on depth of casing, presence of drilling fluid, and time of measurement. Thus, these data are regarded as preliminary and must be used discreetly. There is no correlation between the thickness of the low-velocity zone and these preliminary static water levels. Density-moisture laboratory data from the five drill holes, moreover, show that the degree of saturation in the low-velocity layer ranges from very moist to almost completely saturated. Bogoslovsky and Ogilvy (1977) noted that compressional waves may refract along a ground-water surface, but also noted there is no distinct ground-water table where a landslide body contains clay.

In an idealized, shale-free, poorly consolidated sandstone that is saturated and under heavy static load, the velocity of compressional

waves is averaged through sand grains and pore water (Wyllie, 1963, p. 130). The seismic velocity of water is about 1525 m/s, while that of silica grains is about 5000 m/s. This relationship does not hold, however, in fine-grained to clay-sized near-surface sediments, and the propagation velocity of compressional waves in these media can be much less than that in either the water or the grains (Bailey and Van Alstine, 1973). For example, a seismic line was run several kilometers away from the Springer Ranch landslide through a slough where ground water was within 0.5 m of the ground surface. The velocity of the 100-percent saturated layer, however, was only about half that of water. Evidently, the interstices of very fine-grained rocks that are not heavily loaded are ineffectively connected, so that neither fluid-borne nor grain-borne compressional waves are transmitted efficiently.

In an idealized, unconsolidated quartz sand (shale-free) that is not under heavy load, the compressional-wave velocity will greatly increase when water is added to full saturation, whereas the shear-wave velocity will decrease slightly (Gardner and Harris, 1968). I thus expect the ratio of compressional-wave velocity to shear-wave velocity in the unconsolidated material of the low-velocity layer to increase as water is added, even though the compressional-wave velocity may still be less than that of water.

Shear waves, shear strength, and elastic moduli

The slope at the Springer Ranch landslide has clearly failed in the shear mode to a great extent, and consequently, the slope failure depends on the shearing properties of the slope. A shear-wave line was, therefore, run along line 1 (fig. 5) to help define these shearing properties of both the low- and high-velocity layers.

Shearing strength is defined by the Coulomb equation (Terzaghi and Peck, 1967, p. 103) as shear strength at failure, T_f , by $T_f = c + \sigma \tan \phi$, where c is cohesion, σ is normal stress on the shear plane, and ϕ is internal angle of friction. Cohesion is commonly equated to unconfined compressive strength, q_u at failure in engineering as

$$c = \frac{1}{2} q_u \tan \left(45 - \frac{\phi}{2} \right) ;$$

but for small structures on cohesive soils that are not drained when tested, $c = 0$ and

$$T_f \approx \frac{1}{2} q_u , \quad (1)$$

regardless of the normal stress of overburden. Shear strength obtained by equation 1 is maximum for any test, because ϕ is essentially always greater than zero for a cohesive soil. Imai and Yoshimura (1975) have related shear-wave velocity, V_s , for soils and relatively "soft" rocks to q_u by:

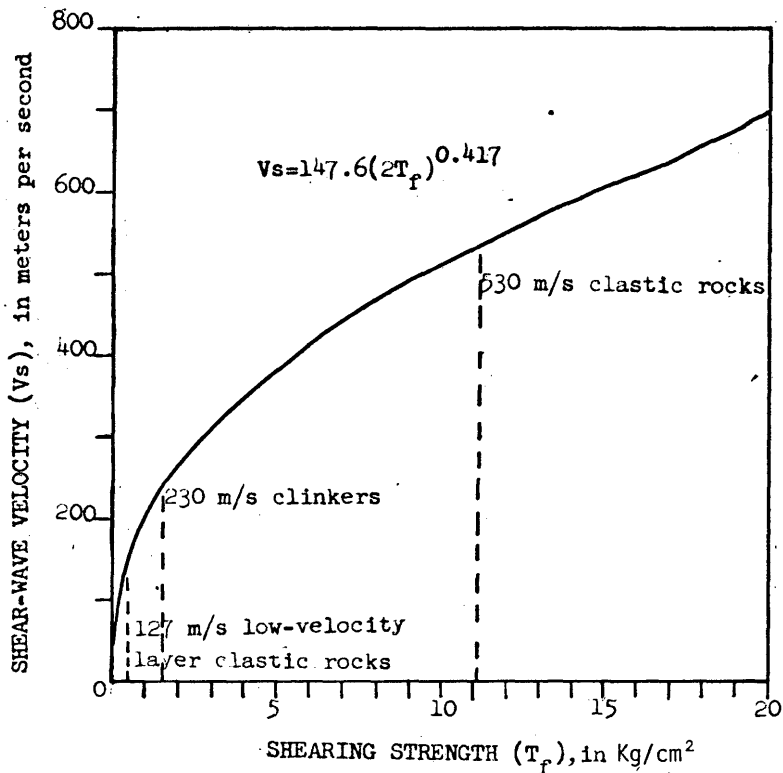
$$V_s = 147.6 q_u^{0.417} . \quad (2)$$

Substituting equation 1 into equation 2,

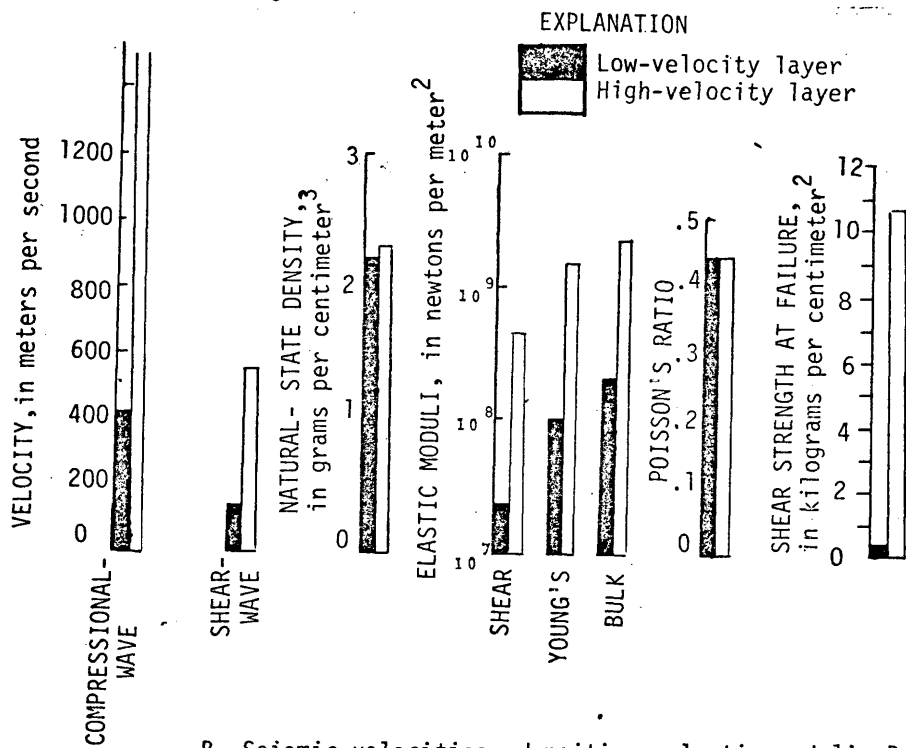
$$V_s \approx 147.6 (2T_f)^{0.417} . \quad (3)$$

Equation 3 is graphed in figure 8, and the shear-wave velocities of both the low- and high-velocity layers are compared as a function of approximate shear strength. The shear strength at failure for the low-velocity layer is about 0.35 kg/cm^3 , while that for the high-velocity layer is about 10.7 kg/cm^3 . Hence, the shear strength of the low-velocity layer is about one-thirtieth that of the high-velocity layer at the landslide.

The elastic moduli and Poisson's ratio (Leet, 1950, p. 38-40; 1960, p. 70-72) are also parameters of relative rock strength, and they were computed from the shear- and compressional-wave velocities and from bulk



A, Shear-wave velocity as a function of approximate shear strength at failure (Imai and Yoshimura, 1975; Terzaghi and Peck, 1967).



B, Seismic velocities, densities, elastic moduli, Poisson's ratio and approximate shear strength at failure for low and high velocity layers.

Figure 8. --Seismic properties of the low- and high-velocity layers of the Springer Ranch landslide.

densities measured on core. The results are summarized in figure 8. These data show that the shear moduli and the other elastic moduli of the low-velocity layer are about one-tenth those of the high-velocity layer.

Because the low-velocity layer is noticeably weaker than the high-velocity layer, and because the interface between the two layers does not show any evidence of having been disturbed, failure within the slope materials is very likely confined to the low-velocity layer. The number and position of main shear planes in the landslide are unknown, but in figure 7 the main slippage surface is assumed to be near the contact between the low- and high-velocity layers. Recent inclinometer data from the slide (A. F. Chleborad, unpub. data, 1978) indicate movement just below the colluvial(?) layer in weathered(?) bedrock.

Landslide model

These seismic investigations imply a shallow-slab landslide in weak earth materials, overlying shaly bedrock, with its toe at a break in the hillside slope, similar to the model described by Krynine and Judd (1957, p. 642-654). Their model has a relatively pervious weathered zone developed over impervious bedrock. If the toe of the potential slide is near a decrease in gradient of the hillside below the toe, then any water introduced into the relatively pervious layer has difficulty discharging at the break in slope, where the gradient decreases. The ground water may or may not be visible at the surface, but in either case a hazardous condition is produced.

Cross section B-B' of figure shows that the toe of the Springer Ranch landslide is at a break in slope. The immediate cause of failure is unknown, but A. F. Chleborad and W. F. Ebaugh (oral commun., 1977)

believe that moisture contributed to the weathered layer is the major factor. The moisture may come from an artesian system beneath the weathered layer, from precipitation on the surface of the layer, or from both. The moisture apparently promoted failure in two ways: (1) it increased pore pressure and lowered the shear strength of the already incompetent low-velocity layer, and (2) it added weight to the low-velocity layer.

Banks of snow have been observed lying on the slope of the Springer landslide. These banks are thickest during spring, and rainfall is greatest during May and June. However, no gullies have been cut through the grass by runoff in the vicinity of the slide, and therefore, much of the meltwater and rain apparently infiltrates rather than running off. Whether or not the hillside becomes saturated, the infiltrating water would greatly increase the weight of the mantle and reduce shear strength, and both changes would promote failure. If the hillside is saturated, though, then pore pressure would be established, and shear strength would decrease further; the pore pressure and seepage forces would be greatest near the toe, where support is effectively decreased, and failure would be promoted.

Summary and conclusions

Landsliding is a geologic hazard to the rapid industrial, commercial, and residential development that is expected in the Powder River Basin. The first section of this report has presented the results of seismic-refraction and shear-wave surveys which are part of a detailed study of the Springer Ranch landslide south-southeast of Sheridan, Wyo. This landslide may be sufficiently representative of

other landslides in the area that the principles learned from it can be applied to the others.

The surveys determined that a low-velocity layer overlies a high-velocity layer, both on the slide and nearby. The seismic velocities of these layers are very similar to those of other clastic rocks in other parts of the basin as well as in the Soviet Union. The low-velocity layer averages 400 m/s at the slide while the high velocity layer averages 1470 m/s. The low-velocity layer defines a relatively weak mantle of colluvium and unconsolidated or weathered bedrock, and the high-velocity layer defines relatively strong, subweathered to nonweathered bedrock. The thickness and configuration of the low-velocity layer were determined using the method of differences, which accounts for variations in thickness of the low-velocity layer. The variations may be due to a change in the surface topography, the topography of the buried contact between the low-velocity and high-velocity layers, or both. The interpreted buried contact is nearly parallel with the restored topographic surface.

The following observations indicate slope failure at the Springer Ranch landslide is confined to the low-velocity layer:

1. The buried contact of the low- and high-velocity layers is relatively smooth and is nearly parallel with the restored topographic surface. There is no indication that any of the high-velocity layer (bedrock) has been displaced or removed. Regional dip of the bedrock is but a few degrees which probably eliminates the possibility of most bedding plane slip surfaces.

2. Shear strength and elastic moduli are both parameters of rock strength. The ratio of the shear strength of the low-velocity layer to the high-velocity layer is approximately 1:30, while the ratio for the elastic moduli is 1:10.

The number and position of main shear planes in the landslide are unknown, but the main slippage surface is assumed to be near the contact between the low- and high-velocity layers.

The major immediate cause of landslide failure is probably the addition of moisture to the low-velocity layer. The moisture apparently promotes failure by increasing pore pressure, lowering shear strength, and adding weight to at least part of the incompetent low-velocity layer.

The predictable similarities of seismic properties between the slide and other parts of the Powder River Basin imply that seismic and engineering geology can be used to help predict or delineate landslides in the basin. Corrective action would be directed at the low-velocity zone and would include avoidance, dewatering, prevention of saturation, buttressing the toe, and unloading the head. The present seismic surveys show that the low-velocity layer on hillsides and over clastic rocks, where it was measured, is less than 5 m thick and may be excavated by dozing, whereas the bedrock must be blasted. This implies that underpinning a structure to nonweathered bedrock or, perhaps, removal of the low-velocity layer prior to construction would be feasible.

CLINKER DEPOSITS

Geology

Clinkers have been studied in many parts of the world, and they are known by a wide variety of names: scoria, baked shale, slag, natural slag, and porcellanite. Clinker deposits, as defined in this report, include all these baked and fused rocks as well as any coke and ash residue from the burned coal. The first descriptions of "burnt earth" in the Missouri River Basin were in the records of the 1804 expedition of Lewis and Clark (Hayden, 1873).

Mode of ignition

The main mode of ignition of coal beds is thought to be spontaneous combustion. Rogers (1917) witnessed burning at six localities, and all of the burns apparently started spontaneously in relatively "fresh" outcrops along small, rapidly cutting streams. Combustion starts at a free surface, more commonly in a thick bed rather than in a thin one. Rogers related, however, accounts of ignition by prairie fires and one account of ignition by man's campfires. He also generally recognized that coals with a moderate to high proportion of volatiles are subject to spontaneous combustion. Finely divided coal is more susceptible to spontaneous ignition than are larger pieces, and small increments of heat are important in the process.

Formation of clinkers

Clinkers in the Powder River Basin are formed from claystones, mudstones, siltstones, shale, and generally fine-grained sandstones of the Fort Union Formation and overlying Wasatch Formation, which are Tertiary in age. Rocks that are superjacent to burned coal beds show variable appearances and properties that are related to original rock

type and degree of alteration. The degree of baking of the rocks decreases with distance from the burned coal bed and, in places, clinker deposits can be traced laterally or upward from highly fused material, to virtually unaltered lignite deposits. Baking and fusing, however, is not seen in the rocks that underlie the burning coal.

Fusing occurs either within a few feet above the burning coal or along fracture-vents that conduct hot gases from the coal to the ground surface. The resulting clinkers are very porous, brittle, and highly fractured. Fine-grained rocks are apparently altered more easily than coarse grained ones. Rogers (1917) suggests that rocks may be fused as much as 23 m above the burning coal. Upon cooling, the fused rocks around the fracture vents form erosion-resistant chimney-like masses. The chimneys are darker colored and harder than the surrounding clinkers, and the radius of chimneys at one excavated site ranged from about 6 to 25 m (R. G. Warburton, Wyoming State Highway Department, written commun., 1976). Clinkers form in the clastic rocks overlying coal beds that have burned. Burning occurs most commonly at outcrops and apparently also under relatively shallow overburden in the Powder River Basin. Extensive coal-exploration drilling done throughout the basin by the Montana Bureau of Mines and Geology, in cooperation with the U.S. Geological Survey, did not penetrate clinkers below a depth of about 30 m (Eldon Woods, oral commun., 1975). Mapel (1959) reports clinkers that are more than 45 m thick east of Buffalo, Wyo. However, C. T. Reid (oral commun., 1976), a driller from Sheridan, Wyo., says that his drill penetrated more than 90 m of clinkers while drilling about 32 km east of Sheridan. Where cover over the coal is more than about 8 m thick in the Powder River Basin, the burning apparently does

not extend more than 60-90 m into the hillside, unless fracture vents form and oxygen is conducted to the fire. Where the cover is less than about 6 m thick or where coal is exposed around buttes or long spurs, the burning can apparently extend much further into the hillside.

Numerous shallow depressions with interior drainage are characteristics of clinker-covered erosion-resistant topographic surfaces. The depressions evidently formed when clinkers slumped into the voids left by the burning coal beds. Lake De Smet, which lies between Sheridan and Buffalo, Wyo., and is more than 5 km long, apparently occupies a depression of this type (Mapel, 1959).

Geotechnical properties

Both exploration and materials testing of clinkers have been done by the Wyoming State Highway Department in the Powder River Basin, according to Jack Hale (written commun., August 16, 1971), E. J. Bauer (written commun., March 23, 1975), and R. G. Warburton (written commun., 1976).

Exploration trenches and holes were excavated by the Department in some clinker deposits with equipment as light as backhoes and augers. Sandstones were mostly altered only to the extent of color change, whereas the clays were more vesicular and glassy, fractured, and darker colored. The relatively harder and stronger clinkers were of the shale type, particularly in the fused-chimney areas. Delineation of the chimneys by trenching, however, was very difficult because of differential alteration and collapse during formation of the clinkers. Warburton concluded that each potential quarrying site for clinkers must be evaluated thoroughly and independently.

The material properties of the clinkers also varied widely because of differential alteration, and the specific gravities, therefore, ranged from 1.85 to 2.25. When samples were compacted in accordance with AASHTO (American Association of State Highway Officials) T-99 they had maximum dry bulk densities of 1.44-1.60 g/cm³ and optimum moisture content ranging from 15 to 25 percent. When the samples were tested according to AASHTO T-180, the maximum dry bulk densities of 1.60-1.76 g/cm³ and optimum-moisture range was 10-20 percent.

The Wyoming State Highway Department considers clinkers to be a very good highway subgrade material if quality control is exercised. They have successfully used crushed clinkers as a cement-treated base in combination with a sand filler and in seal coating of highways. They feel that selectively graded clinkers could be used as a coarse aggregate in concrete pavement provided it was not used as a wearing surface.

Some geotechnical and geophysical tests were also run on clinkers by R. A. Farrow and A. L. Ramirez of the U.S. Geological Survey. The tested properties include hardness, drillability, density, color, and magnetic and seismic properties. These tests were first run at the site east of Gillette, Wyo. (fig. 1), shown by figure 9, and were later repeated on laboratory samples from that site.

Temperature-dependent properties

Most of the tested properties of clinkers are dependent on the temperature during baking and fusing. Figure 10 shows (A) the concept some temperature-dependant properties observed in the field and laboratory and (B) the glass or crystal phase and color of heated shale and alluvial clay (Insley and Frechette, 1955, p. 229-235, after

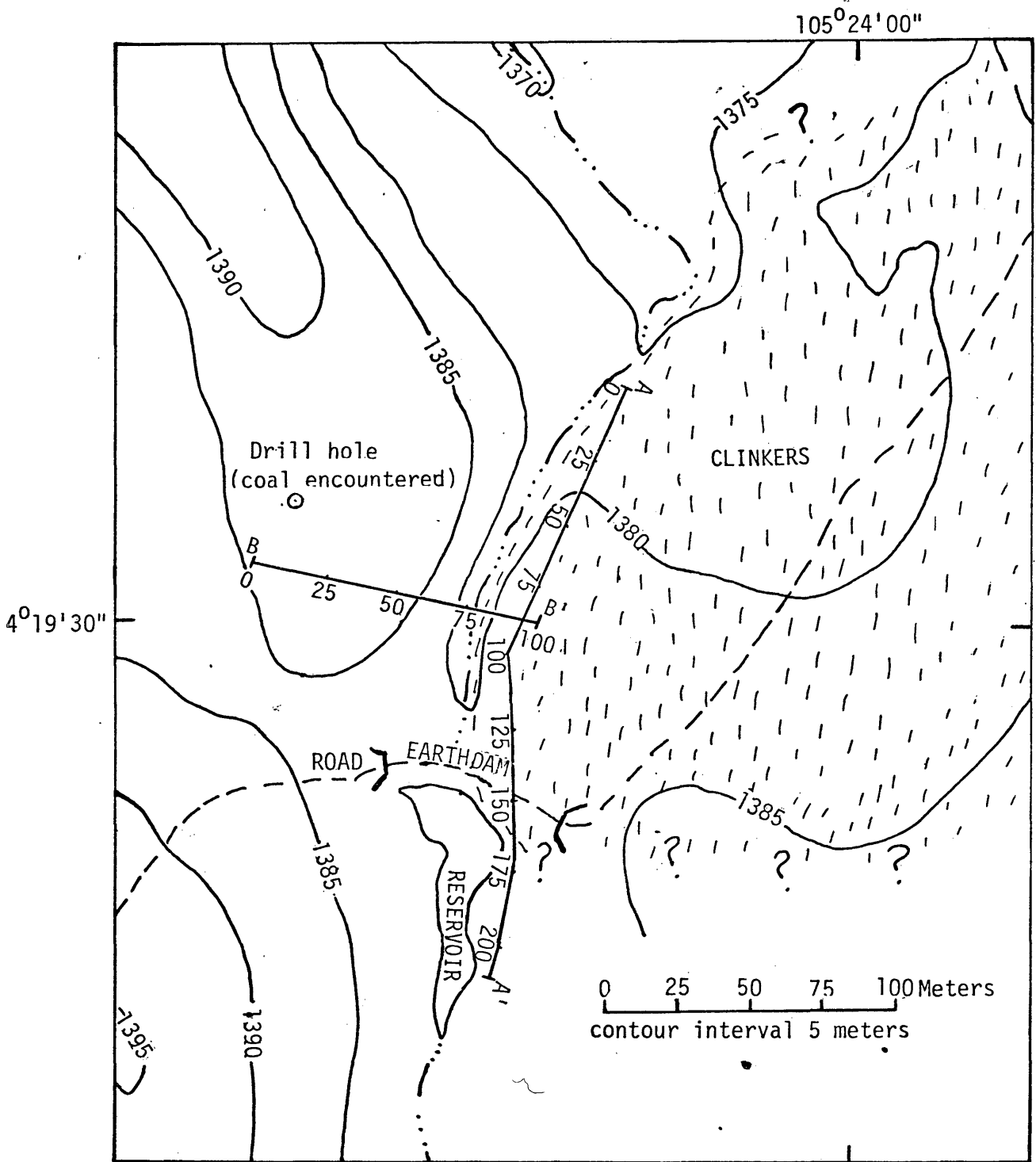
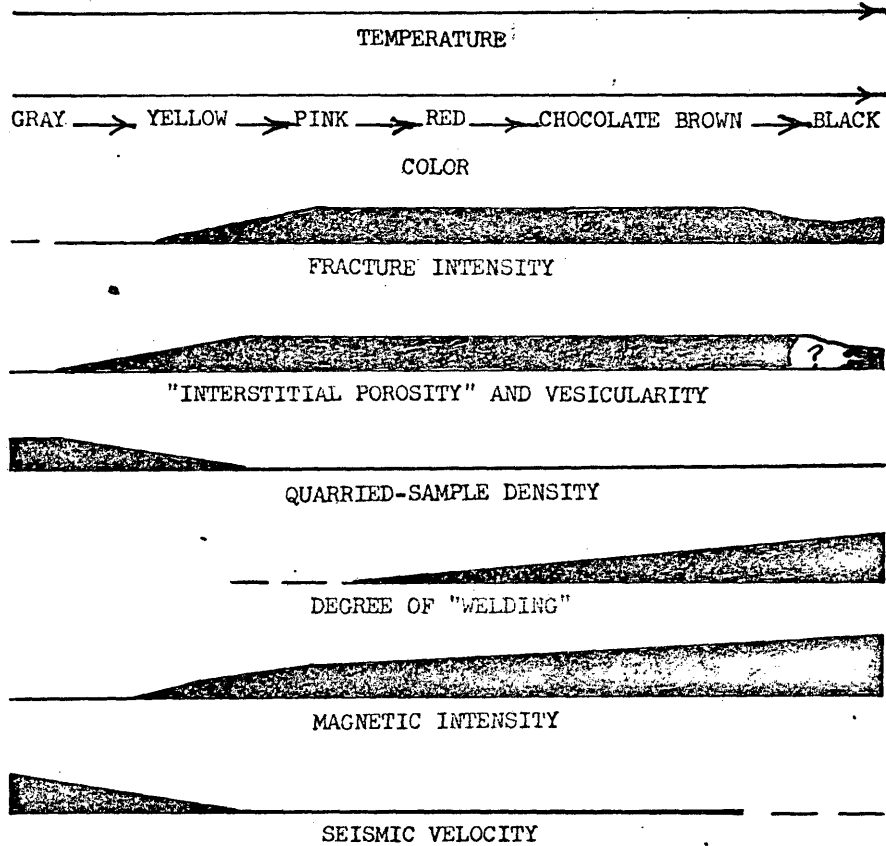
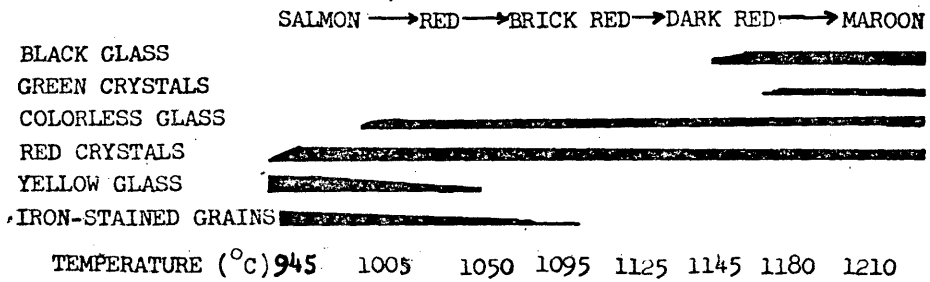


Figure 9- Clinker study area (Fig. 1) showing sites of geotechnical, magnetic, and seismic investigations of clinkers (stippled) near Gillette, Wyoming, along survey lines A-A' and B-B'.



A, Generalized properties of clinkers.



B, Color of glass and crystal phases of shale and alluvial clay (Insley and Frechette, 1955, after G.R. Shelton).

Figure 10- Some properties of clinkers as a function of temperature.

G. R. Shelton). The figures show that as the temperature of "gray," relatively reduced, clastic rocks increases, the rocks are first baked and then fused, and the rock colors correspondingly grade from light to dark. Most of the welding or fusing is done near chimneys, where the heat is intense. Similarly, the dark-colored rocks with high magnetism tend to be near these vents, which are also reducing environments. There is a dramatic increase of fracture intensity, porosity (including vesicularity), and magnetic intensity with increase of temperature accompanied by a rapid decrease in bulk density and seismic velocity. Welding occurs at the higher temperatures.

Density, porosity, and fracture intensity

Densities and porosities were measured in a U.S. Geological Survey laboratory on samples of clinkers from the site east of Gillette, Wyo. The dry bulk densities ranged from 1.56 to 1.87 g/cm³ and averaged 1.68 g/cm³. Porosities ranged from 31 to 39 percent and averaged 36 percent. Average bulk density of nonaltered clastic rocks is about 2.25 g/cm³, and their porosities are about 15-25 percent. The total porosities of rocks measured in place, however, is considerably greater than those measured on samples in the laboratory, because the in situ clinkers display much more fracture porosity than the laboratory samples. The total porosity of most in situ clinker deposits is estimated to be on the order of 50 percent, which is about one-fourth to two-thirds more than that of the laboratory-measured samples.

Clinker samples are quarried only with great difficulty because of their highly fractured nature. An intact sample is, therefore, not representative of an outcrop, and laboratory samples are inherently biased toward the relatively stronger clinkers.

Hardness

Hardness, as used here, implies resistance to deformation. Schmidt rebound hardness (Deere and Miller, 1966) was one kind of field test run on in situ clinkers. This test provides a Schmidt hardness number that is commonly compared to uniaxial compressive strength. These tests were run on fresh clinker surfaces in the outcrop along line A-A' of figure 9. The clinkers, however, were almost completely nonresponsive to the Schmidt hammer tests, and the data were not definitive. Because the clinkers are so highly fractured, it was impractical to core a clinker sample for uniaxial testing.

Drillability

Clinkers were tested for drillability by a test originally developed by Protodyakonov (1963) and modified by Tandanand and Unger (1975). This laboratory test is related to percussion drilling in particular, and the drillability is a function of hardness and wearability as well as other parameters.

The drillability test (fig. 11) generates CRS (Coefficient of Rock Strength) numbers, which are proportional to the minimum number of blows needed to at least partly crush a sample, divided by the maximum volume of minus 0.5-mm material produced by the blows. Of course, the test requires certain normalizing conditions.

The average CRS number from 12 drillability tests on clinkers is compared in figure 11 with CRS numbers of other rock types. The CRS number of the clinkers is the lowest shown. Even so, the CRS number of the clinkers seems high considering that the other types of rocks are relatively competent.

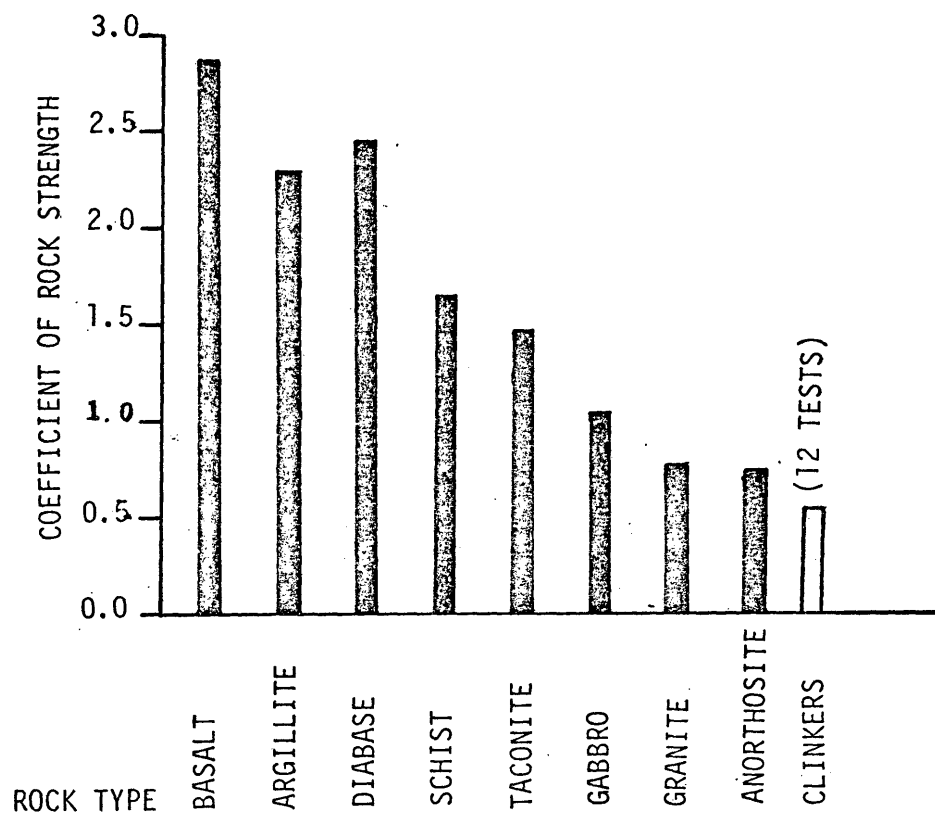


Figure 11. --Coefficient of rock strength of clinkers tested by the U.S. Geological Survey, compared to those of rock types tested by Tandrand and Unger, 1975.

Clinkers are usually rotary drilled, and the drilling is very difficult. The main problems are loss of circulation and caving above the drill bit.

Geophysical properties, clinker study site

Gillette, Wyoming

Magnetic properties

When gray clastic rocks are heated, they tend to turn some shade of red or dark brown and become more magnetic. According to D. E. Watson (unpub. data, 1976) the reddish color can be mostly attributed to iron-oxide silicates, but the minerals that mainly contribute to the thermal-remanent magnetism are generally found to be ilmenohematites and titanomagnetites. The magnetic domains of these minerals are originally in a relatively random orientation, but heating reorients the domains so that they are parallel with the Earth's field at the time of the heating; thus, the net magnetization is greatly enhanced. The temperature does not have to exceed the Curie point, however, for the rocks to be remagnetized. Partial reheating is sufficient to realine many of the magnetic grains. Near the chimneys, however, the rocks tend to be much more magnetic. This is due to exposure to extremely high temperatures, which are frequently above the Curie temperatures of most minerals, and to the presence of slightly reducing gases, which keep the minerals from oxidizing to the more weakly magnetic hematite, for instance.

Comparison of the distribution of magnetization of various rock types is shown in figure 12. The net magnetization of a clastic rock is dramatically increased by several orders of magnitude when the rock is baked, and the strength of magnetization appears to relate to the degree of baking and fusing. The resulting clinkers are among the most

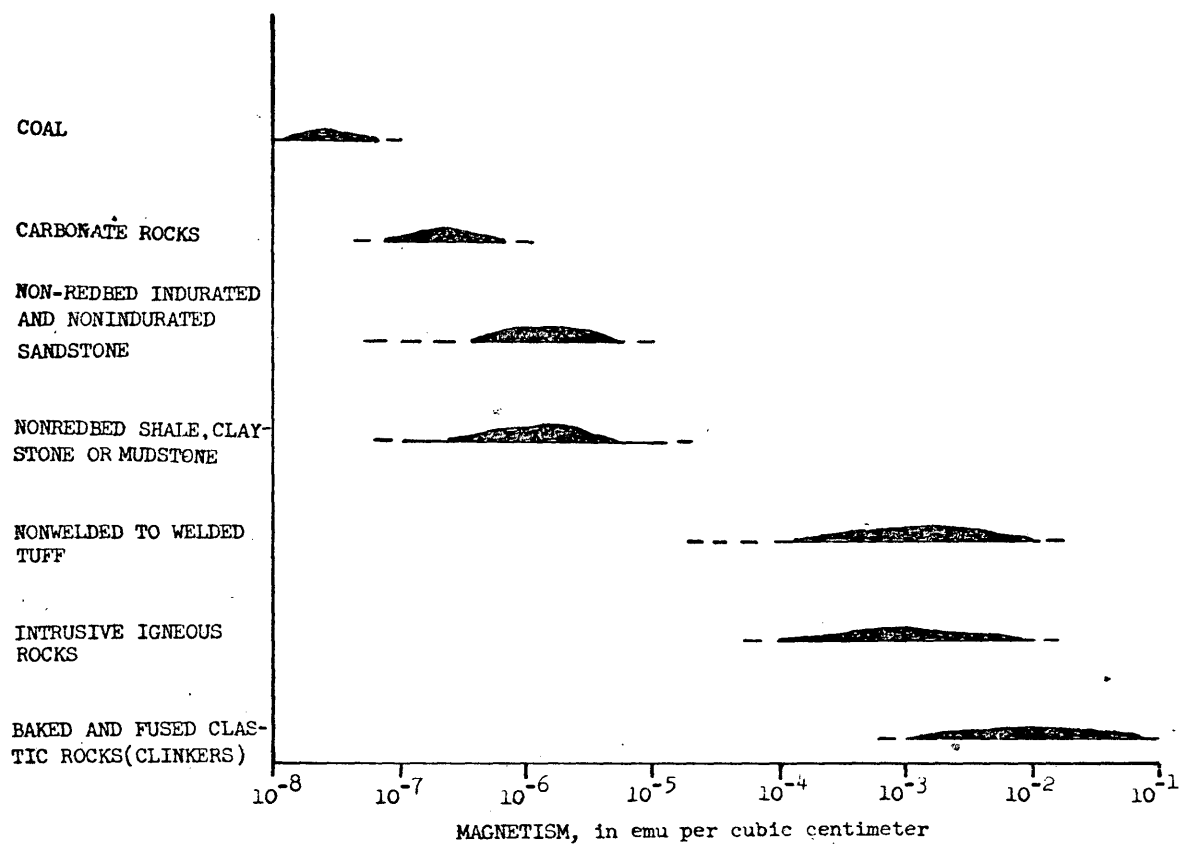


Figure 12- Representative net magnetism of various rock types (D.E. Watson, unpublished data, 1976).

magnetic rocks found in nature. This great magnetization is the basis of the present investigations of the lateral extent of buried clinker deposits.

Magnetic survey.--Magnetic surveys were run with a portable proton magnetometer at the Gillette, Wyo., clinker study site (fig. 9) along lines A-A', in conjunction with seismic and geotechnical surveys, and along line B-B'. Readings were taken at about 3-m intervals with the sensor at a constant height of about 2.1 m above the ground. Individual readings of total magnetic intensity were read to an accuracy of about ± 1 gamma (1 nanotesla). The readings were reduced to a base value of 58,595.0 gammas, which is representative of the Earth's total intensity magnetic field near Gillette, Wyo. Base readings were repeated within 15 minutes of the initial reading at an accuracy of ± 4 gammas, and this base drift was linearly distributed over the station readings.

The magnetic survey run along line B-B' (fig. 13) defines the extent of the clinkers, which crop out east of the streambed. Only small amounts of clinkers can be seen in the colluvium derived from clastic rocks along the west bank. Although traces of coal cannot be seen in the colluvium along the west bank, coal cuttings are visible at the collar of a drill hole about 80 m west of the stream. A magnetic anomaly of more than 700 gammas is shown over the clinker outcrop. The anomaly begins at about 45 m west of the stream and achieves greatest magnitude over the crown of the outcrop of clinkers. The midpoint of the anomaly is nearly over the streambed. Secondary, higher-frequency

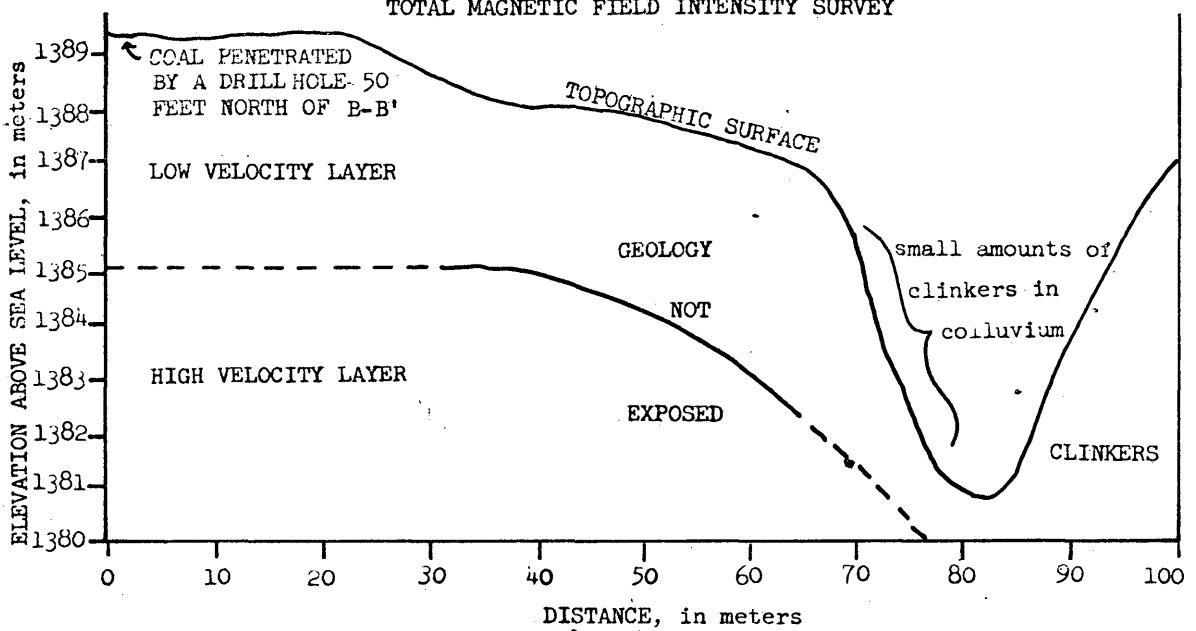
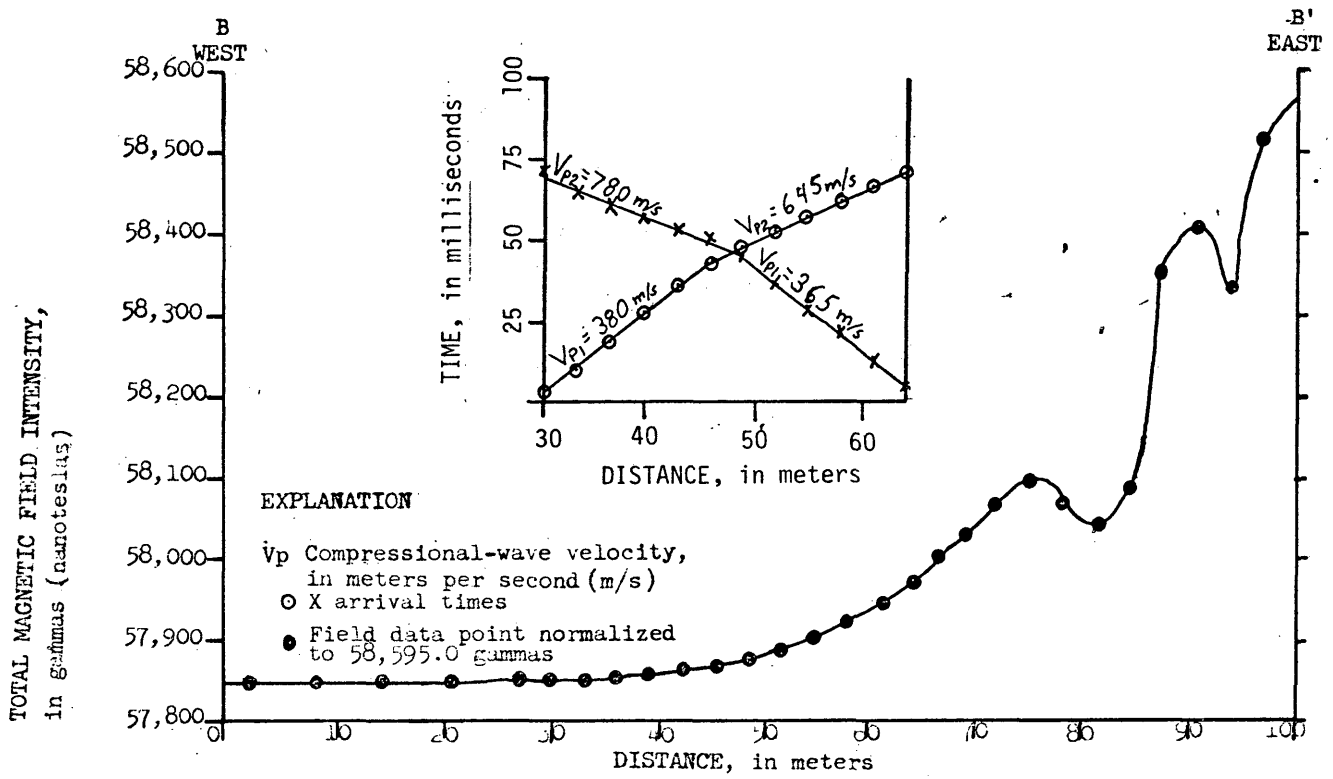


Figure 13- Magnetic field intensity (normalized to 58,595.0 gammas) and seismic surveys along B-B' (fig. 9)

inflections are on the flank of the main magnetic anomaly. These seem to be caused mostly by higher frequencies due to a steep gradient of magnetization.

If the midpoint along the flank of the major anomaly is chosen as the contact of clinkers and clastic rocks, it would be approximately at the streambed. Presumably, the burn began somewhere along the east side of the young, rapidly cutting stream, because the clinker deposit apparently ends near the streambed. The midpoint method for determining the edge of clinkers is apparently accurate to within about 2 m.

This method of exploration for a lateral contact of clinkers with coal or clastic rocks was first described by Hasbrouck and Hadsell (1976). They demonstrated the relative ease of location of buried clinkers if only one seam has burned and found that the method is useful for locating clinker quarries, water wells, and other construction sites and for planning seismic exploration surveys. Conversely, the method is useful for determining coal reserves by delineating the edge of unburned coal deposits without extensive drilling.

Magnetic line A-A' (fig. 14) was run parallel to the clinker outcrop to determine the magnetic field of the exposed clinkers. The cross section along A-A' shows a general anomaly over the outcrop of about 800 gammas, and the magnetic profile indicates that the clinkers probably terminate near the north end of the line. Three or four localized high anomalies of as much as 500 gammas are superimposed on the main anomaly. These localized anomalies probably are affected by subsurface features behind the outcrop and may be caused by highly magnetized chimneys. Only one chimney, about 10-15 ft wide, is exposed (at about 61 m, fig. 14), and there is a localized anomaly associated

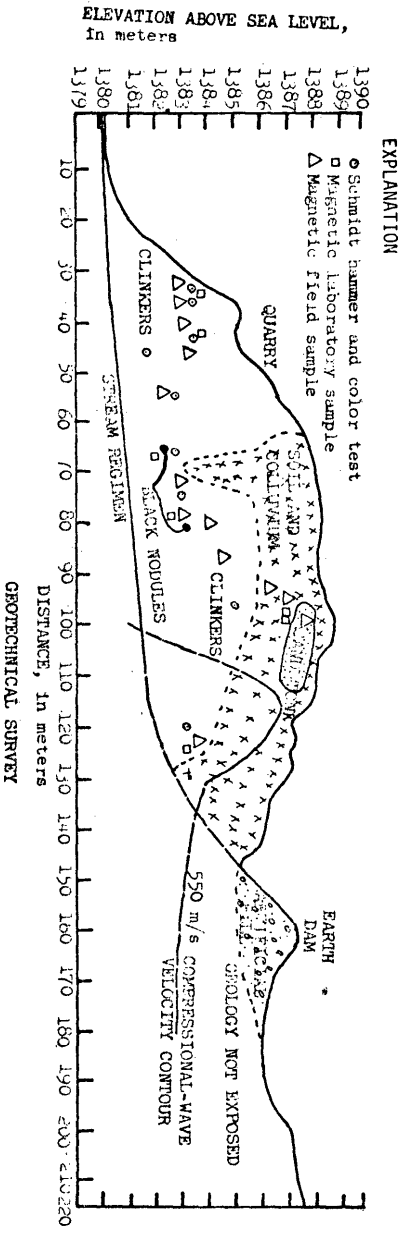
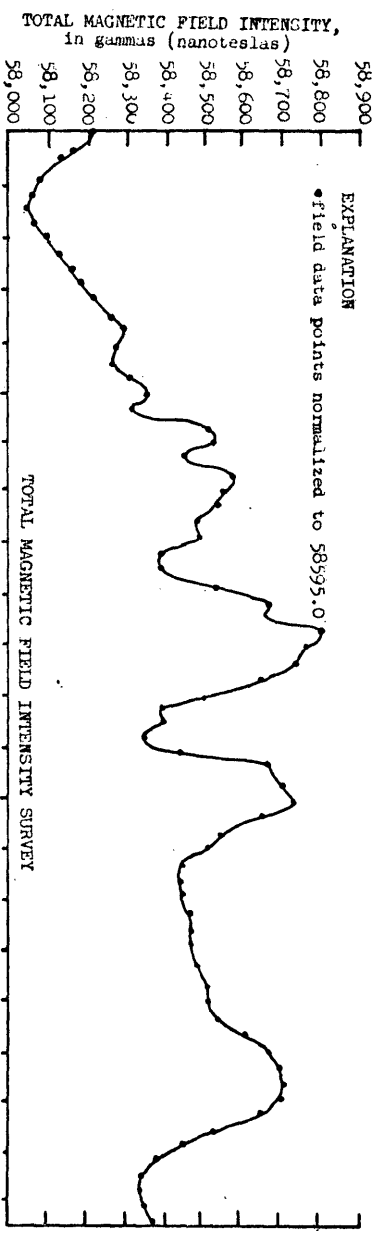
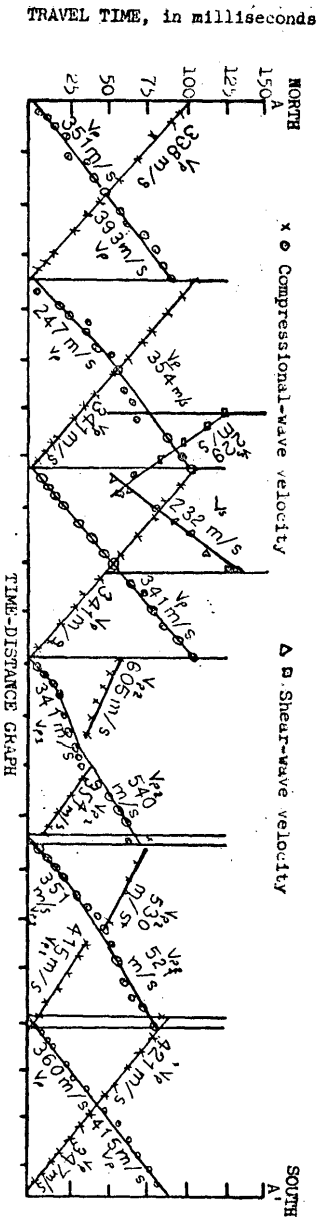


Figure 14- Geotechnical, magnetic, and seismic surveys along A-A' (fig. 9)

with it. D. E. Watson and M. L. Botsford (unpub. data, 1976) have run magnetic profiles near clinker quarries, and have also recorded these localized anomalies. They think that the anomalies are caused either by the fused rocks in chimneys or, perhaps, by random but large variations in magnetization.

Measurements of hand samples compared to the results of laboratory and field surveys.--Remanent magnetism was measured on hand samples with a portable magnetometer, using a field technique described by Briener (1973). These measurements are compared in figure 15 with remanent magnetism measured in the laboratory on two small cores and with the total magnetic field intensity along line A-A' (figs. 9, 14). Neither the hand nor core measurements compare well with the relative amplitude of the magnetic field survey over the outcrop. The laboratory measurements on the two cores, however, compare well with those on hand samples that were selected from the outcrop near the sites where the laboratory samples were selected. Six cores were submitted for laboratory analysis, but four of the samples fractured so badly during preparation that a suitable plug could not be drilled. I conclude that the field hand-sample technique is much faster and convenient, and perhaps as accurate as that of the laboratory core-measuring technique.

Seismic properties

Seismic surveys were run along lines A-A' (fig. 14) and B-B' (fig. 13) at the clinker site (fig. 9). The surveys along A-A' were apparently all on clinkers, while the survey along B-B' was mostly on clastic rocks for comparison to clinkers. The average velocity of the low-velocity layer of clinkers is 344 m/s, which is very similar to that

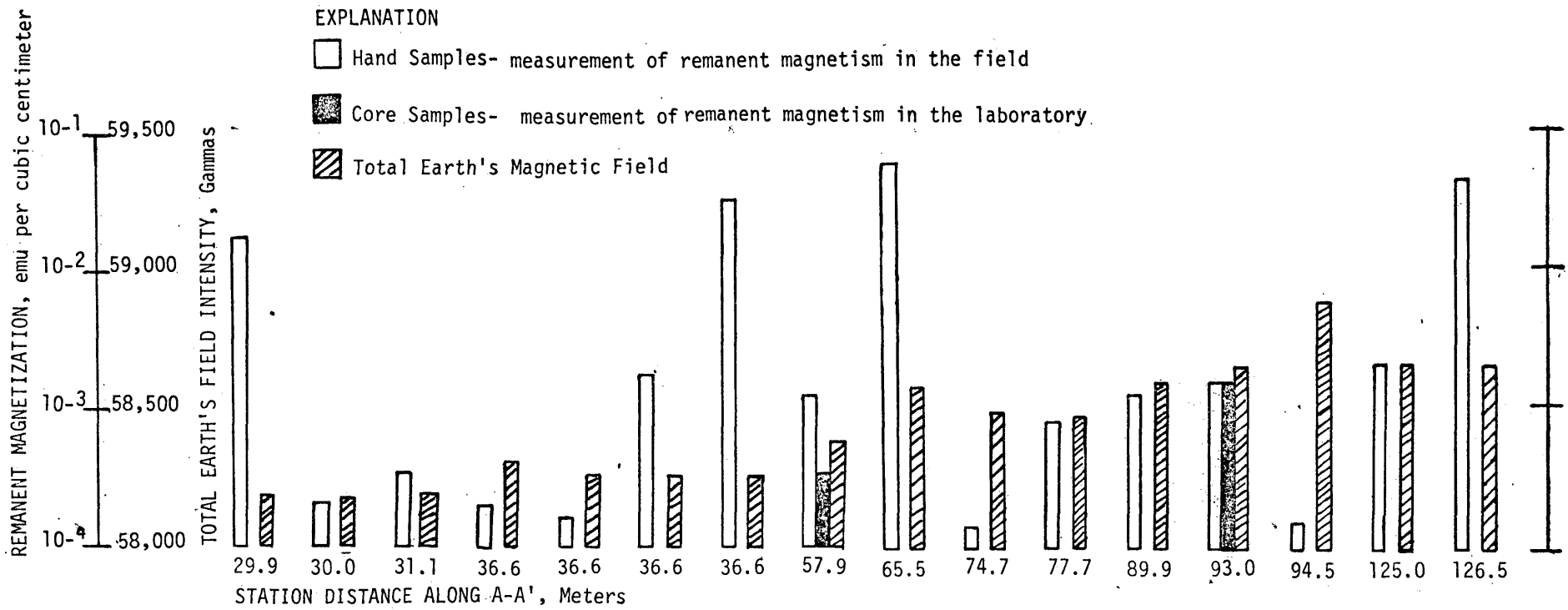


Figure 15- Measurements of remanent magnetism and Earth's total magnetic field intensity on clinkers along line A-A' (fig. 9, 14).

of 372 m/s for the clastic rocks. The average velocity of the high-velocity layer of clinkers, however, apparently averages about 490 m/s, although that of clastic rocks is 712 m/s.

The high-velocity layer of clastic rocks along B-B', however, is poorly developed, and its velocity is exceptionally low for clastic rocks. Perhaps the coal beneath B-B' is weathered enough in the high-velocity zone to account for the anomalously low velocity.

The range of compressional-wave velocity compared to the economical excavation graph of figure 4 indicates that the clinkers in the low-velocity layer may be easily dozed, and that ripping and blasting are not necessary. Clinkers in the high-velocity layer may be marginally dozed and easily ripped, and blasting is not necessary. In practice, however, clinkers in the Powder River Basin are quarried with equipment lighter than a D-7 tractor, although sandstone overburden must sometimes be loosened by explosives. The fused chimney material is also economically dozed, but it is quarried and crushed with much more difficulty than the clinkers that are merely baked. The chimneys, however, are not visually apparent from the level ground surface, but the success of quarrying with light equipment or of siting heavy structures on clinkers may depend on the presence of chimneys (Farooqui and others, 1977).

A small chimney was observed at about 61.0 m along line A-A'. This chimney is not discernible in the seismic data, but the diameter of the chimney is only 1-2 m. I speculate, however, that because chimneys in general are harder than the surrounding baked rocks, they have higher seismic velocities. If the diameter of a roughly circular chimney is a

few meters or more, it may possibly be detected by seismic refraction methods as well as by magnetic methods.

Although the compressional-wave velocities of the low-velocity layers of both the clinkers and clastic rocks are similar, the shear-wave velocities in these same layers are different. The shear-wave velocities of the clinkers are higher than those of the low-velocity layer over clastic rocks (table 1). Furthermore, there is no shear-wave velocity layering apparent in the clinkers. The velocities and texture of the clinkers are compared to those of the clastic rocks and overburden in figure 5, and the shear strengths (at failure) are compared in figure 8. Shear strength of the clinkers is greater than that of the low-velocity layer of clastic rocks but less than that of the high-velocity layer.

The shear-wave velocities of the clinkers indicate some reasons why they do not readily exhibit slope failure. The clinkers are coarsely textured and have a high angle of internal friction. They are, therefore, relatively well drained and have approximately five times the shear strength of the low-velocity layer of clastic rocks.

Most manmade structures experience some settlement. Differential settlement beneath a structure, however, produces failure in the shear mode, first in the earth and then in the structure. The low-velocity layer, which overlies clastic rocks in some towns in the basin, clearly supports heavy structures such as grain silos and bridge abutments, but these structures apparently settle evenly. Even though the clinkers have higher shear strengths than the low-velocity layer over clastic rocks, the clinkers include relatively strong chimneys that may cause differential settlement.

Laboratory measurements compared to field measurements.--Seismic velocities of samples of clinkers along line A-A' were also measured in the laboratory. Compressional- and shear-wave velocities were measured on nine samples, and their elastic moduli and Poisson ratio's are compared in figure 16 with the equivalent field measurements. Shear-wave velocities were measured in the field only in the interval between 60 and 90 m along line A-A'.

Comparison of the laboratory-measured velocities of clinkers with those measured on clinkers in place shows the laboratory samples are much stronger. The reason for the disparity is that the high frequency of fracturing in clinkers in place is not indicated by the laboratory measurements. Intact samples are always chosen for these laboratory tests so that they may be cored. Consequently, the laboratory-derived velocities are heavily biased toward relatively stronger clinkers.

The compressional-wave velocities of the laboratory rock samples (fig. 16) range from 1830 to 4310 m/s and average 2490 m/s, compared to 420 m/s for in situ measurements--a ratio of about 6:1. If the velocities of laboratory rock samples were entered in the method-of-excavation graph (fig. 4), then excavation by blasting or marginal ripping with large tractors would be erroneously indicated.

Summary and conclusions

Many coal beds in the Powder River Basin have burned along their outcrops, and the resulting intense heat has baked and fused the overlying clastic rocks into clinkers. The extent that the coal has burned into the subsurface is not necessarily apparent from the surface, but magnetic methods can delineate the edge of a single layer of buried clinkers. Location of the edge is very important in estimating

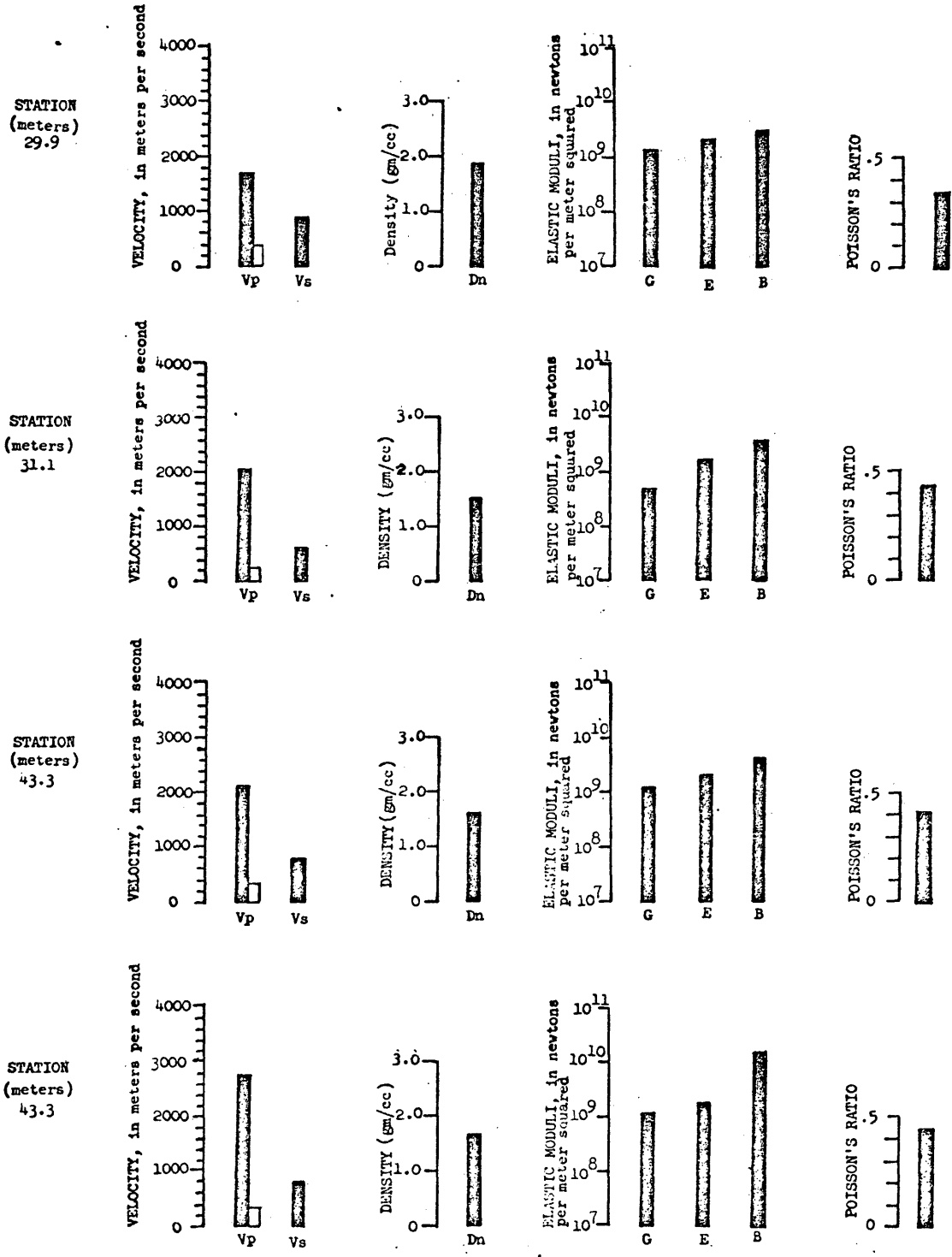
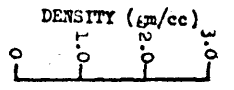
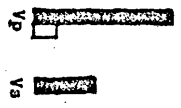
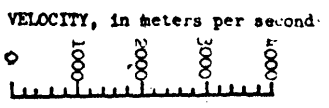
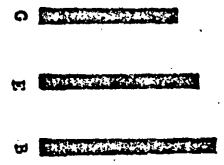
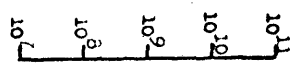


Figure 16. --In situ (open) and laboratory (shaded) measurements of compressional- (Vp) and shear- (Vs) wave velocities, the dynamic-elastic moduli (E = Young's, G = shear, and B = bulk), and Poisson's ratio (σ) run on clinkers along A-A' (figs. 9, 14). (Figure continues on next page).

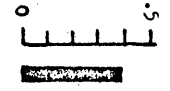
STATION
(meters)
43.3



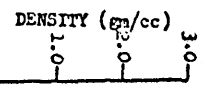
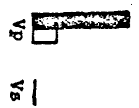
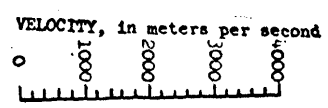
ELASTIC MODULI, in newtons
per meter squared



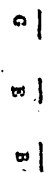
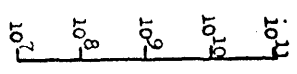
POISSON'S RATIO



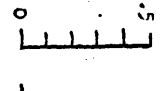
STATION
(meters)
54.9



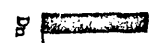
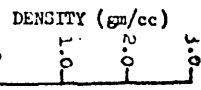
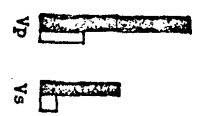
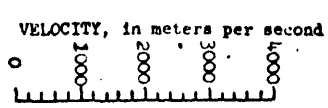
ELASTIC MODULI, in newtons
per meter squared



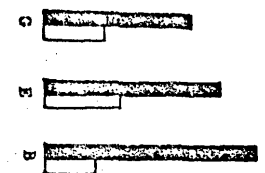
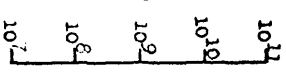
POISSON'S RATIO



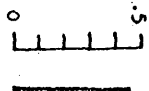
STATION
(meters)
65.8



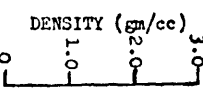
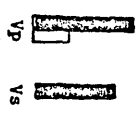
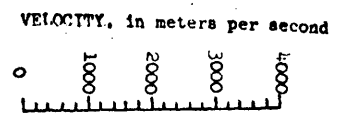
ELASTIC MODULI, in newtons
per meter squared



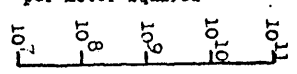
POISSON'S RATIO



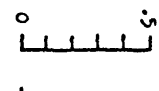
STATION
(meters)
121.9



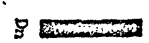
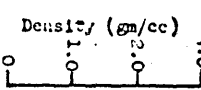
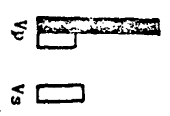
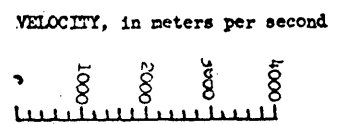
ELASTIC MODULI, in newtons
per meter squared



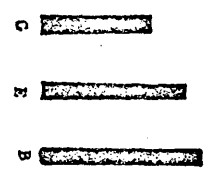
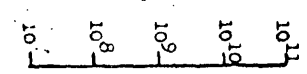
POISSON'S RATIO



STATION
(meters)
124.4



ELASTIC MODULI, in newtons
per meter squared



POISSON'S RATIO

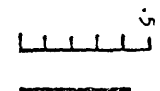


Figure 16. --continued.

nonburned coal deposits, locating clinker quarries, and planning drilling or seismic reflection lines for projects whose success may depend on the absence of clinkers.

The clinkers are very porous and highly fractured, and their erosion-resistant qualities belie their relatively low strength. In much of the basin, however, the clinkers are the only hard material available for building highways and railroads and for use as lightweight aggregate, even though they are weak relative to most other building stone and aggregate. Compressional-wave velocities and observation of quarrying operations show the clinkers can easily be mined without heavy equipment. Drilling and blasting are not necessary, except to loosen some overlying clastic rocks. Compressional-wave velocities done in the laboratory, however, are inherently biased. Only intact samples can be selected for testing, and hence the laboratory erroneously indicates that the clinkers must be loosened either by blasting or, perhaps, by heavy ripping tractors.

The approximate shear strength of the clinkers is five times that of the low-velocity layer overlying clastic rocks but is only one-sixth that of the clastic rocks themselves. Landslides in the basin do not readily occur along slopes of clinkers. Some reasons for this relative slope stability include the coarse texture of the clinkers, which promotes relatively good drainage and permits a high angle of repose, and the greater shear strength of the clinkers, compared to that of the low-velocity layer associated with clastic rocks.

Heavy structures such as coal silos and bridge abutments may have to be sited on clinkers. Differential settlement with failure in the shear mode may occur, however, because chimneys of relatively greater

strength occur within the clinkers. Special foundation-preparation techniques may, therefore, have to be used or, perhaps, chimneys in a single layer of clinkers can be located by geophysical methods and avoided at the construction site. Preliminary investigations indicate that the chimney rocks may be more magnetic, and they are known to be harder than the surrounding clinkers. Consequently, I think that chimneys may be located by measuring three-dimensional magnetic fields and, perhaps, by closely spaced seismic refraction lines.

Remanent magnetism measurements on hand samples in the field may be as accurate as those made in the laboratory. The measurements on hand samples are much faster and more efficient because the highly fractured clinkers are very difficult to prepare for the laboratory tests.

There is no apparent correlation between change in remanent magnetization along the outcrop and changes in total intensity of the Earth's field along the same outcrop.

REFERENCES

- Bailey, A. D., and Van Alstine, C. L., 1973, A downhole shear wave and soils study: Sacramento, California, Nimbus Instruments, 13 p.
- Bauer, L. P., 1972, The alteration of sedimentary rocks due to burning coal in the Powder River Basin, Campbell County, Wyoming: Texas Tech University, M.S. thesis, 65 p.
- Bogoslovsky, V. A., and Ogilvy, A. A., 1977, Geophysical methods for the investigation of landslides: Geophysics, v. 42, no. 3, p. 562-571.
- Briener, Sheldon, 1973, Applications manual for portable magnetometers: Sunnyvale, California, Geometrics, 62 p.
- Caterpillar Tractor Company, 1972, Caterpillar performance handbook [6th ed.]: Peoria, Illinois, Caterpillar Tractor Co. Press, 29 secs.
- Chleborad, A. F., Nichols, T. C., Jr., and Ebaugh, W. F., 1976, A preliminary inventory, description, and statistical evaluation of landslides in a region of projected urban development, Sheridan, Wyoming: U.S. Geological Survey Open-File Report 76-571, 105 p.
- Darracott, B. W., 1976, Seismic surveys and civil engineering: The civil engineer of South Africa, p. 35-40.
- Deere, D. U., and Miller, R. P., 1966, Engineering classification and index properties for intact rock: Available from U.S. Department of Commerce National Technical Information Service, Springfield, Virginia 22161, as report AFWL-TR-65-116, p. 162-171.
- Ebaugh, W. F., 1976, Surficial and bedrock geologic map of the Big Horn quadrangle, Wyoming: U.S. Geological Survey Miscellaneous Field Studies Map MF-801, 1:24,000, 1 sheet.
- _____, 1977, Landslide-factor mapping and slope-stability analysis of the Big Horn quadrangle, Sheridan County, Wyoming: Boulder, Colorado University Ph. D. thesis, 194 p.

- Farooqui, S. M., Deacon, R. J., and Kent, R. C., 1977, Geology of combustion metamorphosed strata near Decker, Montana [abs.]: Seattle, Washington, Association of Engineering Geologists, 20th Annual Meeting, p. 4.
- Farrow, R. A., 1976, Preliminary report on the geotechnical properties of the Wasatch Formation at Buffalo, Wyoming: U.S. Geological Survey Open-File Report 76-877, 78 p.
- Gardner, G. H. F., and Harris, M. H., 1968, Velocity and attenuation of elastic waves in sands, in Transactions of the Society of Professional Well Log Analysts, Ninth Annual Logging Symposium, Houston, Texas: p. 1-19.
- Hasbrouck, W. P., and Hadsell, F. A., 1976, Geophysical exploration techniques applied to western United States coal deposits, in Coal exploration: 1st International Coal Exploration Symposium, London, England, 1976, Proc., 664 p.
- Hayden, F. V., 1873, A report of progress for the year 1872 embracing portions of Montana, Idaho, Wyoming, and Utah: U.S. Geological Survey, 6th Annual Report, p. 358-359.
- Imai, Tsuneo, and Yoshimura, Masayoshi, 1975, The relation of mechanical properties of soils to P- and S-wave velocities for soil ground in Japan: Oyo Technical Note 07, 15 p.
- Insley, Herbert, and Frechette, Van Derck, 1955, Microscopy of ceramics and cements, including glasses, slags and foundry sands: New York, Academic Press, 286 p.
- Krynine, D. P., and Judd, W. R., 1957, Principles of engineering geology and geotechnics: New York, McGraw-Hill, p. 637-671.

- Laby, T. H., 1931, The principles and practice of geophysical prospecting, in Edge, A. B. B., ed., Imperial geophysical experimental survey: Cambridge, England, Cambridge University Press, p. 637-671.
- Leet, L. D., 1950, Earth waves: Cambridge, Mass., Harvard Monographs in Applied Science, no. 2, 122 p.
- _____ 1960, Vibrations from blasting rock: Cambridge, Mass., Harvard University Press, 134 p.
- Lowry, M. E., and Cummings, T. R., 1966, Ground-water resources of Sheridan County, Wyoming: U.S. Geological Survey Water-Supply Paper 1807, 77 p.
- Mapel, W. J., 1959, Geology and coal resources of the Buffalo-Lake De Smet area, Johnson and Sheridan Counties, Wyoming: U.S. Geological Survey Bulletin 1078, 148 p. [1961].
- Miller, C. H., and Bullard, T. F., 1978a, Elastic constants, in Catalog of contributed programs: Corvallis, Oregon, Hewlett Packard 65 Users Library, Program 05374-A, 5 p.
- _____ 1978b, Stadia-alidade traverse reductions, in Catalog of contributed programs: Corvallis, Oregon, Hewlett Packard 65 Users Library, Program 05393-A, 5 p.
- _____ 1978c, Depth and configuration of a buried refraction-velocity layer, in Catalog of contributed programs: Corvallis, Oregon, Hewlett Packard 65 Users Library, Program 05394-A, 5 p.
- Protodyakonov, M. M. 1963, Mechanical properties and drillability of rocks in Fairhurst, C., ed, 5th Symposium on Rock Mechanics, Minnesota University, May 1962, Proc.: New York, Macmillan, p. 103-118.

- Redpath, B. B., 1973, Seismic refraction exploration for engineering site investigations: U.S. Army Corps Engineers Technical Report E-73-4, 51 p.
- Rogers, G. S., 1917, Baked shale and slag formed by the burning of coal beds: U.S. Geological Survey Professional Paper 108, 10 p.
- Tandanand, Sathit, and Unger, H. F., 1975, Drillability determination--a drillability index for percussion drills: U.S. Bureau of Mines Report of Investigations 8073, 20 p.
- Terzaghi, Karl, and Peck, R. B., 1967, Soil mechanics in engineering practice: John Wiley and Sons, 729 p.
- Wyllie, M. R. J., 1963, The fundamentals of well log interpretation [3d ed.]: New York, Academic Press, 238 p.

Appendix I

Hewlett Packard 65 Programs:

1. Depth and configuration of a buried refraction-velocity layer
2. Elastic constants
3. Stadia-alidade traverse reductions



- New Program
- Revision to Program No. _____

HP-65 Serial No. 1606 A 01723

Program Title DEPTH and CONFIGURATION of a buried REFRACTION-VELOCITY LAYER
Underline 1 or 2 Keywords

Keyword(s) 1 REFRACTION-VELOCITY
Underlined in Title
 2 DEPTH and CONFIGURATION

No. of Steps 99

Category No. 05.05

Category Name Earth Sciences

Abstract- 75 Word Maximum Distances and arrival times from a seismic refraction survey are used to calculate the depth and configuration of a buried velocity layer of a two-layer case by both the Time-Intercept and the Differences methods. Input units can be in either the metric or English systems and output units are in the same system as those of input.

Name	CARTER THOMAS <small>First</small>	H. F. <small>Initial</small>	MILLER BULLARD <small>Last</small>
Address	U.S. Geological Survey, Br. of Engineering Geology, MS 903, Box 25046		
City	Denver	State	Colorado Zip Code 80225

Program Choice: Enter number of program you would like to receive if your program is accepted into the library.

First Choice Alternate Choice

Submittal Checklist: Please use the checklist below to insure submittal of all the proper program documentation.

- | | |
|--|---|
| <input checked="" type="checkbox"/> Program Submittal | <input checked="" type="checkbox"/> HP-65 User Instructions |
| <input checked="" type="checkbox"/> Program Description I | <input checked="" type="checkbox"/> HP-65 Program Form(s) |
| <input checked="" type="checkbox"/> Program Description II | <input checked="" type="checkbox"/> Magnetic Card (s) |

ACKNOWLEDGMENT AND AGREEMENT

To the best of my knowledge, I have the right to contribute this program material without breaching any obligation concerning nondisclosure of proprietary or confidential information of other persons or organizations. I am contributing this program material on a nonconfidential nonobligatory basis to Hewlett-Packard Company ("HP") for inclusion in its program library, and I agree that HP may use, duplicate, modify, publish, and sell the program material, and authorize others to do so without obligation or liability of any kind. HP may publish my name and address, as the contributor, to facilitate user inquiries pertaining to this program material.

Signature _____ Date _____



Program Title Depth and configuration of a buried refraction-velocity layer

Contributor's Name Carter H. Miller and Thomas F. Bullard

Address U.S. Geological Survey, Br. of Engineering Geology, MS 903, Box 25046

City Denver State Colorado Zip Code 80225

Program Description, Equations, Variables, etc.

INPUT:

Average velocity, \bar{V}_1 , of the first layer,
 Updip apparent velocity, V_u , of the second layer,
 Downdip apparent velocity, V_d , of the second layer,
 Travel time, T_{ab} (in msec), from either shot point to the farthest seismometer,
 Time intercept, T_u (in msec), of the V_u curve projected to distance zero,
 Time intercept, T_d (in msec), of the V_d curve projected to distance zero,
 Travel time, T_a (in msec), from shot point No. 1 through the V_2 layer to a given seismometer,
 Travel time, T_b (in msec), from shot point No. 2 through the V_2 layer to the same seismometer used for T_a .

OUTPUT:

Angle, i_c (decimal degrees), of a seismic ray to \bar{V}_1-V_2 , the interface between velocity layers,
 Angle, α (decimal degrees), of the slope of \bar{V}_1-V_2 ,
 True velocity, V_2 , of the buried velocity layer,
 Depth, Z_u , of the \bar{V}_1-V_2 interface at its deepest place along the seismic line (T_u end),
 Depth, Z_d , of the shallowest place (T_d end) along the seismic line,
 Depth(s), h , of the \bar{V}_1-V_2 interface under all seismometers at times T_a and T_b where V_u overlaps V_d .

FORMULAS:

$$Z_u = \frac{\bar{V}_1 T_u}{2 \cos i_c}, \quad Z_d = \frac{\bar{V}_1 T_d}{2 \cos i_c}, \quad h = \frac{\bar{V}_1 (T_a + T_b - T_{ab})}{2 \cos i_c}$$

Operating Limits and Warnings

Velocities may be input in either the English or metric system; output units are in the same system as those of the input.

Steps must follow in the order A, B, C, D, E, followed by computations of "h."
 $V_2 > V_1$; $V_u > V_d$; $Z_u > Z_d$; $V_2 \neq (V_u + V_d)/2$.

Tab "forward shooting" \approx Tab "reverse shooting" for shallow shot points.

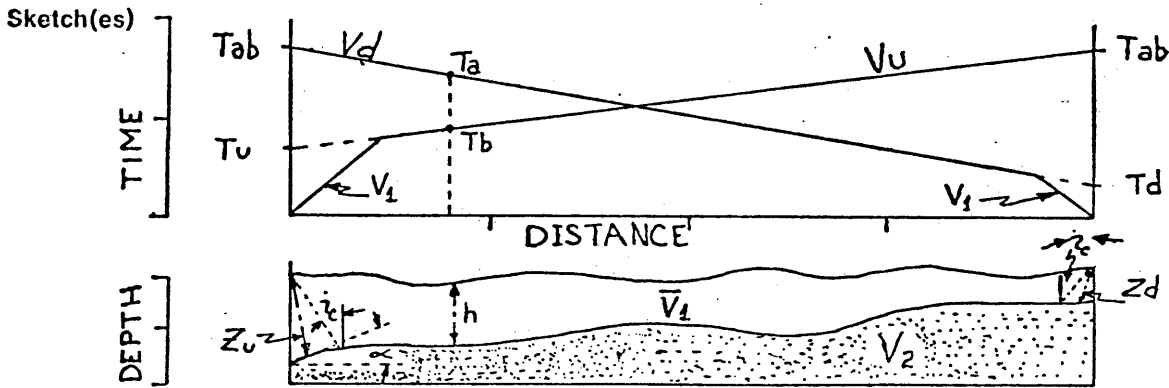
T_a and T_b must be travel times from opposite ends of the seismic line through the V_2 layer and detected at the same seismometer.

The depths Z_u and Z_d are perpendicular distances from the \bar{V}_1-V_2 plane to the ground-surface plane, whereas h distance(s) is from the undulating \bar{V}_1-V_2 contact to the

undulating ground surface.

This program has been verified only with respect to the numerical example given in *Program Description II*. User accepts and uses this program material AT HIS OWN RISK, in reliance solely upon his own inspection of the program material and without reliance upon any representation or description concerning the program material.

NEITHER HP NOR THE CONTRIBUTOR MAKES ANY EXPRESS OR IMPLIED WARRANTY OF ANY KIND WITH REGARD TO THIS PROGRAM MATERIAL, INCLUDING, BUT NOT LIMITED TO, THE IMPLIED WARRANTIES OF MERCHANTABILITY AND FITNESS FOR A PARTICULAR PURPOSE. NEITHER HP NOR THE CONTRIBUTOR SHALL BE LIABLE FOR INCIDENTAL OR CONSEQUENTIAL DAMAGES IN CONNECTION WITH OR ARISING OUT OF THE FURNISHING, USE OR PERFORMANCE OF THIS PROGRAM MATERIAL.



Sample Problem(s) A seismic refraction survey was conducted in order to determine the depth to a buried layer and its configuration. After constructing a time-distance graph, the following data are determined:

- $\bar{V}_1 = 370$ m/s,
- $V_u = 985$ m/s,
- $V_d = 955$ m/s,
- $T_{ab} = 45.05$ m sec,
- $T_u = 14.0$ m sec,
- $T_d = 13.7$ m sec

Using the time-intercept method, compute the critical angle, i_c , the angle of dip, α , the true velocity of V_2 , in m/s, and the depths Z_u and Z_d , in meters.

Using the method of differences, compute the depths, h , under each recording station where the V_u and V_d curves overlap with the following sets of T_a and T_b , in m sec:

- $T_{a1} = 23.1, T_{b1} = 35.4; T_{a2} = 26.5, T_{b2} = 31.9; T_{a3} = 27.5, T_{b3} = 28.2;$
- $T_{a4} = 27.4, T_{b4} = 31.9; T_{a5} = 25.1, T_{b5} = 36.0.$

Solution(s) 370 [R/S] 985 [R/S] 955 [R/S] 45.05 [R/S] 14.0 [R/S] 13.7 [R/S]

- [A] ----- 22.43° i_c , critical angle
- [B] ----- 0.34° α , dip angle
- [C] ----- 969.77 m/s, V_2
- [D] ----- 2.8 m, Z_u
- [E] ----- 2.74 m, Z_d

23.1 [R/S] → 35.4 [R/S]	- - - 2.69 m, h	27.4 [R/S] → 31.9 [R/S]	- 2.85 m, h
26.5 [R/S] → 31.9 [R/S]	- - - 2.67 m, h	25.1 [R/S] → 36.0 [R/S]	- 3.21 m, h
27.5 [R/S] → 28.2 [R/S]	- - - 2.13 m, h		

Reference(s) Time-Intercept Method: Dobrin, M. B., 1976, Introduction to Geophysical Prospecting: 2d ed., McGraw-Hill, New York, p. 292-338.
 Method of Differences: Laby, T. H., 1931, The principles and practice of geophysical prospecting: Report of the Imperial Geophysical Survey, Cambridge, England, p. 337-41. Hollister, J. C., 1957, Modification of the method of differences: written communication, Colorado School of Mines. Redpath, B. B., 1973, Seismic refraction for engineering site investigations: U.S. Army Engineer Waterways Experiment Station, Explosive Excavation Research Laboratory, Livermore, Calif 55 n



HP-65 Program Form

TCH TO W/PRGM. PRESS PRGM TO CLEAR MEMORY.

Y RY	CODE SHOWN	COMMENTS	KEY ENTRY	CODE SHOWN	COMMENTS	REGISTERS
	23		SIN	04	α	R ₁ \bar{V}_1
	00		R/S	84		
	84		LBL	23	Computes V_2	
1	33 01	V_1	C	13		R ₂ V_u
	84		RCL 1	34 01		
2	33 02	V_u	RCL 7	34 07		
	84		f	31		R ₃ V_d
3	33 03	V_d	SIN	04		
	84		\div	81	V_2	
0 4	33 04	T_{ab}	\rightarrow R/S	84		R ₄ T_{ab}
	84		LBL	23	Computes Z_u	
5	33 05	T_u	D	14		
	84		RCL 1	34 01		R ₅ T_u
6	33 06	T_d	2	02		
	84		\div	81		
	23	Computes critical	RCL 7	34 07		R ₆ T_d
	11	angle, i_c	f	31		
1	34 01		COS	05		
2	34 02		\div	81		R ₇ i_c
	35		\rightarrow STO 8	33 08		
	04		RCL 5	34 05		
	71		x	71		R ₈ \bar{V}_1
8	33 08	$V_1/2 \cos i_c$	EEX	43		$2 \cos i_c$
1	34 01		3	03		
3	34 03		CHS	42		R ₇ 10^{-3}
	35		STO 7	33 07		
	04		x	71	Z_u	
	71		R/S	84		LABELS
	61		LBL	23	Computes Z_d	A i_c
	83		\rightarrow E	15		B α
	05		RCL 8	34 08		C V_2
	71		RCL 6	34 06		D Z_u
	32		x	71		E Z_d
	04		RCL 7	34 07		0
7	33 07	i_c	x	71	Z_d	1 h
	84		LBL	23	Computes h	2
	23	Computes dip angle, α	1	01		3
	12		R/S	84		4
8	34 08		ENTER	41		5
IS	42		\rightarrow R/S	84		6
1	34 01		+	61		7
3	34 03		RCL 4	34 04		8
	35		-	51		9
	04		RCL 8	34 08		
	71		x	71		FLAGS
	61		RCL 7	34 07		1
	83		x	71		
	05		GTO	22		2
	71		1	01		
-1	32		100			



New Program

Revision to Program No.

HP-65 Serial No. 1 6 0 6 A 0 1 7 2 3

Program Title E l a s t i c C o n s t a n t s
Underline 1 or 2
Keywords

Keyword(s) 1 E l a s t i c
Underlined
in Title 2 C o n s t a n t s

No. of Steps 9 8

Category No. 0 5 . 0 5

Category Name E a r t h S c i e n c e s

Abstract- 75 Word Maximum When compressional- and shear-wave velocities and bulk-density values are supplied, the program calculates the elastic moduli and Poisson's ratio. Input is in meters per second and output is in both pounds per square inch and Newtons per square meter.

Name and Thomas ^{First} Carter ^{Initial} H. F. ^{Last} Miller Bullard
Address U.S. Geological Survey, Branch of Engineering Geology, MS 903, Box 25046,
Denver Federal Center
City Denver State Colorado Zip Code 80225

Program Choice: Enter number of program you would like to receive if your program is accepted into the library.

0 0 3 6 0 A
First Choice Alternate Choice

Submittal Checklist: Please use the checklist below to insure submittal of all the proper program documentation.

- Program Submittal
- Program Description I
- Program Description II
- HP-65 User Instructions
- HP-65 Program Form(s)
- Magnetic Card (s)

ACKNOWLEDGMENT AND AGREEMENT

To the best of my knowledge, I have the right to contribute this program material without breaching any obligation concerning nondisclosure of proprietary or confidential information of other persons or organizations. I am contributing this program material on a nonconfidential nonobligatory basis to Hewlett-Packard Company ("HP") for inclusion in its program library, and I agree that HP may use, duplicate, modify, publish, and sell the program material, and authorize others to do so without obligation or liability of any kind. HP may publish my name and address, as the contributor, to facilitate user inquiries pertaining to this program material.

Signature _____ Date _____



Program Title ELASTIC CONSTANTS

Contributor's Name Carter H. Miller and Thomas F. Bullard

Address U.S. Geological Survey, Branch of Engineering Geology, MS 903, Box 25046, DFC

City Denver State Colorado Zip Code 80225

Program Description, Equations, Variables, etc. This program calculates elastic moduli and Poisson's ratio when provided with the following data:

compressional wave velocity, V_p in m/s ,

shear wave velocity, V_s in m/s ,

bulk density, D_b in gm/cm³, where

shear modulus, $G = V_s^2 D_b$, in psi and N/m² ,

Poisson's ratio, $\sigma = \frac{.5(V_p^2/V_s^2) - 1}{(V_p^2/V_s^2) - 1}$,

Young's Modulus, $E = 2G(1 + \sigma)$, in psi and N/m²,

bulk modulus, $B = \frac{E}{3(1 - 2\sigma)}$, in psi and N/m².

Operating Limits and Warnings. The moduli must be computed in the sequence shown in Program Description II and User Instructions.

N/m² does not necessarily need to be computed. If a modulus is read in psi, and N/m² is not desired, simply key the next label.

After all moduli are computed, any modulus or ratio may be recalled by keying the appropriate label.

If you err or wish to restart in mid-program, key GTO, 0, R/S, and then key in the new V_p , V_s , and D_b .

If you wish to enter velocities in feet per second delete the following program steps: 6, 7, 8, 9, 10, 11, 12, 17, and 18.

This program has been verified only with respect to the numerical example given in Program Description II. User accepts and uses this program material AT HIS OWN RISK, in reliance solely upon his own inspection of the program material and without reliance upon any representation or description concerning the program material.

NEITHER HP NOR THE CONTRIBUTOR MAKES ANY EXPRESS OR IMPLIED WARRANTY OF ANY KIND WITH REGARD TO THIS PROGRAM MATERIAL, INCLUDING, BUT NOT LIMITED TO, THE IMPLIED WARRANTIES OF MERCHANTABILITY AND FITNESS FOR A PARTICULAR PURPOSE. NEITHER HP NOR THE CONTRIBUTOR SHALL BE LIABLE FOR INCIDENTAL OR CONSEQUENTIAL DAMAGES IN CONNECTION WITH OR ARISING OUT OF THE FURNISHING, USE OR PERFORMANCE OF THIS PROGRAM MATERIAL.



Sketch(es)

Sample Problem(s)

Calculate the shear modulus, G , in psi and N/m^2 , Poisson's ratio, σ , Young's modulus, E , in psi and N/m^2 , and the bulk modulus, B , in psi and N/m^2 for a material with the following properties:

compressional wave velocity, $V_p = 2,100$ m/s

shear wave velocity, $V_s = 945$ m/s

bulk density, $D_b = 2.05$ gm/cm³

Solution(s)	2,100	[R/S]	945	[R/S]	2.05	[R/S]
[A]	→	2.66×10^5	psi (G)			
[R/S]	→	1.83×10^9	N/m^2 (G)			
[B]	→	3.73×10^{-1}	(σ)			
[C]	→	7.29×10^5	psi (E)			
[R/S]	→	5.03×10^9	N/m^2 (E)			
[D]	→	9.57×10^5	psi (B)			
[R/S]	→	6.60×10^9	N/m^2 (B)			

Reference(s)

Leet, L. D., 1950, Earth waves, Harvard Monographs in Applied Science, no. 2, Cambridge, Mass., Harvard University Press.



INSTRUCTIONS	INPUT DATA/UNITS	KEYS	OUTPUT DATA/UNITS
Enter program card		<input type="text"/> <input type="text"/>	
Initialize		GTO,0 R/S	
Enter Vp	Vp, m/s	R/S <input type="text"/>	Vp ² f/s
Enter Vs	Vs, m/s	R/S <input type="text"/>	Vs ² f/s
Enter Db	Db, gm/cm ³	R/S <input type="text"/>	
Compute shear modulus, G		A <input type="text"/>	GX10 ⁶ psi
		R/S <input type="text"/>	GX10 ⁹ N/m ²
Compute Poisson's ratio, sigma		B <input type="text"/>	sigma
Compute Young's modulus, E		C <input type="text"/>	EX10 ⁶ psi
		R/S <input type="text"/>	EX10 ⁹ N/m ²
Compute bulk modulus, B		D <input type="text"/>	BX10 ⁶ psi
		R/S <input type="text"/>	BX10 ⁹ N/m ²
		<input type="text"/> <input type="text"/>	
		<input type="text"/> <input type="text"/>	
		<input type="text"/> <input type="text"/>	
		<input type="text"/> <input type="text"/>	
		<input type="text"/> <input type="text"/>	
		<input type="text"/> <input type="text"/>	
		<input type="text"/> <input type="text"/>	
		<input type="text"/> <input type="text"/>	
		<input type="text"/> <input type="text"/>	
		<input type="text"/> <input type="text"/>	
		<input type="text"/> <input type="text"/>	
		<input type="text"/> <input type="text"/>	
		<input type="text"/> <input type="text"/>	
		<input type="text"/> <input type="text"/>	
		<input type="text"/> <input type="text"/>	
		<input type="text"/> <input type="text"/>	
		<input type="text"/> <input type="text"/>	
		<input type="text"/> <input type="text"/>	
		<input type="text"/> <input type="text"/>	
		<input type="text"/> <input type="text"/>	
		<input type="text"/> <input type="text"/>	
		<input type="text"/> <input type="text"/>	
		<input type="text"/> <input type="text"/>	
		<input type="text"/> <input type="text"/>	
		<input type="text"/> <input type="text"/>	
		<input type="text"/> <input type="text"/>	
		<input type="text"/> <input type="text"/>	

For a new case, program returns automatically to step 3 after completing step 9. Simply key new Vp, Vs, and Db data. To abort in mid-program, re-initialize (step 2) and key in new data.

If you desire to enter velocities in f/s instead of m/s, delete the following program steps: 6, 7, 8, 9, 10, 11, 12, 17, and 18.

SWITCH TO W/PRGM. PRESS f PRGM TO CLEAR MEMORY.

KEY ENTRY	CODE SHOWN	COMMENTS	KEY ENTRY	CODE SHOWN	COMMENTS	REGISTERS
BL	23		STO 5	33 05		R ₁ 3.281
0	00		2	02		
R/S	84		÷	81		
OSP	21		1	01		R ₂ Vp ²
4	04		-	51		
3	03		RCL 5	34 05		
.	83		1	01		R ₃ Vs ²
2	02		-	51		
8	08		÷	81		
1	01		⁶⁰ STO 7	33 07		R ₄ Db
0 1	33 01		R/S	84	σ	
X	71		LBL	23	Computes Young's modulus, E	
ITER↑	41		C	13		R ₅ (Vp/Vs)
X	71		RCL 7	34 07		
0 2	33 02		1	01		
R/S	84		+	61		R ₆ G
L 1	34 01		RCL 6	34 06		
X	71		X	71		
ITER↑	41		2	02		R ₇ σ
X	71		⁷⁰ X	71		
0 3	33 03		STO 8	33 08		
R/S	84		R/S	84	EX10 ⁵ psi	R ₈ E
0 4	33 04		6	06		
R/S	84		8	08		
BL	23	Computes shear modulus	9	09		R ₉
A	11	G	5	05		
L 3	34 03		X	71		
.	83		R/S	84	EX10 ⁹ N/m ²	LABELS
0	00		LBL	23	Computes bulk modulus	A G
1	01		⁸⁰ D	14	B	B σ
3	03		RCL 8	34 08		C E
4	04		3	03		D B
7	07		÷	81		E
5	05		RCL 7	34 07		0
X	71		2	02		1
L 4	34 04		X	71		2
X	71		CHS	42		3
0 6	33 06		1	01		4
R/S	84	GX10 ⁶ psi	+	61		5
6	06		⁹⁰ ÷	81		6
8	08		R/S	84	BX10 ⁶ psi	7
9	09		6	06		8
5	05		8	08		9
X	71		9	09		
R/S	84	GX10 ⁹ N/m ²	5	05		FLAGS
BL	23	Computes Poisson's ratio, σ	X	71	BX10 ⁹ N/m ²	1
B	12		GTO	22		2
L 2	34 02		0	00		
L 3	34 03					
÷	81					



New Program

Revision to Program No. 00140 A

HP-65 Serial No. 1606 A 01723

Program Title STADIA-ALIDADE TRAVERSE REDUCTIONS
Underline 1 or 2
Keywords

Keyword(s) 1 STADIA-ALIDADE
Underlined
In Title 2 REDUCTIONS

No. of Steps 96

Category No. 99.03

Category Name SURVEYING

Abstract- 75 Word Maximum The described program reduces stadia intervals and middle-hair readings in any units, and also reduces vertical angles, which are referenced to 30° on an alidade, into difference of elevation between the alidade and the surveyed point. Absolute elevation of either the instrument or the surveyed point is also determined when backsight or foresight is keyed, and the results are stored for the next sighting in the traverse. True horizontal or slope distances may also be optionally computed for any sighting.

Name Carter
Thomas
First

H.
F.
Initial

Miller
Bullard
Last

Address U.S. Geological Survey, Br. of Engineering Geology, MS 903, Box 25046

City Denver State Colorado Zip Code 80225

Program Choice: Enter number of program you would like to receive if your program is accepted into the library.

First Choice

Alternate Choice

Submittal Checklist: Please use the checklist below to insure submittal of all the proper program documentation.

- Program Submittal
- Program Description I
- Program Description II
- HP-65 User Instructions
- HP-65 Program Form(s)
- Magnetic Card(s)

ACKNOWLEDGMENT AND AGREEMENT

to the best of my knowledge, I have the right to contribute this program material without breaching any obligation concerning disclosure of proprietary or confidential information of other persons or organizations. I am contributing this program material on nonconfidential nonobligatory basis to Hewlett-Packard Company ("HP") for inclusion in its program library, and I agree that HP may use, duplicate, modify, publish, and sell the program material, and authorize others to do so without obligation or liability of any kind. HP may publish my name and address, as the contributor, to facilitate user inquiries pertaining to this program material.

Signature _____ Date _____



Program Description I

Program Title Stadia-Alidade Traverse Reductions

Contributor's Name Carter H. Miller and Thomas F. Bullard

Address U.S. Geological Survey, Br. of Engineering Geology, MS 903, Box 25046
 Denver State Colorado Zip Code 80225

Program Description, Equations, Variables, etc.
 The formulas:

Difference of Elevation = $\frac{\text{Observed Distance} \times \sin^2(\text{vertical angle})}{2}$,

True Horizontal Distance = Observed Distance $\times \cos^2(\text{vertical angle})$,

True Slope Distance = Observed Distance $\times \cos(\text{vertical angle})$,

BM = Bench Mark

I = Instrument Station

BS = Backsight

FS = Foresight

M-Hair = Middle Hair

I.I. = Height of Instrument

Diff. Elev. = Difference in Elevation

Elev. Instr. = Elevation of Instrument

Elev. Ground = Elevation of Ground

Horiz. Dist. = True Horizontal Distance

Stadia Constant = 100.0

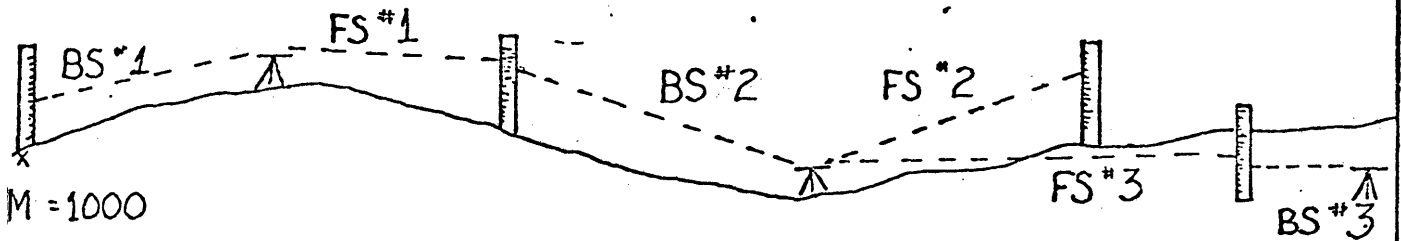
Operating Limits and Warnings Input stadia interval (any unit is acceptable) not stadia distance. Angles are keyed in with a decimal point separating degrees and minutes-seconds; e.g., 31°45'30" is input as "31.4530"; for level sights input 30°00'00" as

The last elevation of the plane table (a backsight) is stored in R₅; it remains there until [A] (BS key) is used again; therefore, any number of foresights can be made from one instrument setup. The last elevation of the ground under the plane table (a foresight) is stored in R₁ and this elevation is made available for the next backsight. If a mistake occurs in mid-program, restart by keying [GTO], [0], [R/S], and inputting the last accurate ground elevation in R₁. Then continue with the next backsight.

This program has been verified only with respect to the numerical example given in Program Description II. User accepts and uses program material AT HIS OWN RISK, in reliance solely upon his own inspection of the program material and without reliance on any representation or description concerning the program material.

NEITHER HP NOR THE CONTRIBUTOR MAKES ANY EXPRESS OR IMPLIED WARRANTY OF ANY KIND WITH REGARD TO THIS PROGRAM MATERIAL, INCLUDING, BUT NOT LIMITED TO, THE IMPLIED WARRANTIES OF MERCHANTABILITY AND FITNESS FOR A PARTICULAR PURPOSE. NEITHER HP NOR THE CONTRIBUTOR SHALL BE LIABLE FOR INCIDENTAL OR CONSEQUENTIAL DAMAGES IN CONNECTION WITH OR ARISING OUT OF THE FURNISHING, USE OR PERFORMANCE OF THIS PROGRAM MATERIAL.

Sketch(es)



The following data were obtained from a plane-table and alidade survey:

Station	Stadia Interval	M-Hair	Vertical Angle	Diff. Elev.	Horiz. Dist.	Elev. Instr.	Elev. Ground	Remarks
BS #1	12.3	10.0	27°31'					BM elev.=1000 H.I.=1.2
FS #1	11.0	10.0	28°00'					True Slope Dist. = 1099.3
BS #2	10.4 (12.0)	1.0 (1.0)	31°25' (31°00')	()	()	()	()	"Side Shot"
FS #2	11.1	5.3	30°00'					
BS #3	10.9	6.1	30°00'					

From the given information compute the differences in elevation between the ground point at the rod and the instrument; compute the absolute elevations of the instrument on backsights and the ground on foresights, compute the True Horizontal Distance from the instrument to rod station, and, if desired, compute True Slope Distance from instrument to rod.

Station(s) 1000 STO 1 12.3 R/S 10 R/S 27.31 R/S → - 53.2, Diff. Elev. BS #1
 1063.2, Elev. Instr. BS #1 C → 1227.7, True Horiz. Dist.
 11.0 R/S 10 R/S 28.0 R/S → -38.4, Diff. Elev. FS #1
 1014.9, Elev. Ground FS #1 C → 1098.7, True Horiz. Dist.
 1099.3, True Slope Dist.
 10.4 R/S 1.0 R/S 31.25 R/S → 25.7, Diff. Elev. BS #2
 990.2, Elev. Instr. BS #2 C → 1039.4, True Horiz. Dist.
 12.0 R/S 1.0 R/S 31.0 R/S → 20.9, Diff. Elev. FS #2
 1010.1, Elev. Ground FS #2 C → 1199.6, True Horiz. Dist.
 11.1 R/S 5.3 R/S 30.0 R/S → 0, Diff. Elev. FS #3
 984.9, Elev. Ground FS #3 C → 1110, True Horiz. Dist.
 10.9 R/S 6.1 R/S 30 R/S → 0, Diff. Elev. BS #3
 991.0, Elev. Instr. BS #3 C → 1090, True Horiz. Dist.

Reference(s) Low, J. W., 1957, Geologic field methods: Harper and Bros., New York, p.

U.S. Geological Survey, 1963, Stadia tables for obtaining differences of elevation: -342, 41 p.

I wish to thank R. A. Farrow, C. R. Dunrud, and A. F. Chleborad for reviewing this program.



HP-65 Program Form

CH TO W/PRGM. PRESS PRGM TO CLEAR MEMORY.

KEY	CODE SHOWN	COMMENTS	KEY ENTRY	CODE SHOWN	COMMENTS	REGISTERS
	23		GTO	22		R ₁ Elev.
	00		0	00		Ground
	84		LBL	23		
	01		B	12	Computes Elev. Ground	R ₂ Dist.
	00		0	00		
	00		RCL 4	34 04		
	71		gx<y	35 22		R ₃ M-Hair
2	33 02	Observed Dist.	GTO	22		
	84		2	02		
3	33 03	M-Hair	60 RCL 3	34 03		R ₄ Diff. Elev.
	84		-	51		
	32		RCL 5	34 05		
IS	03		+	61		R ₅ Elev. Instr.
	03		STO 1	33 01	Elev. Ground	
	00		GTO	22		
	51		0	00		R ₆ Vertical Angle
6	33 06	Vertical Angle	LBL	23		
	02		2	02		
	71		RCL 3	34 03		R ₇
	31		70 CHS	42		
	04		+	61		
2	34 02		RCL 5	34 05		R ₈
	71		+	61		
	02		STO 1	33 01		
	81		GTO	22		R ₉
4	33 04		0	00		
	84	Diff. Elev.	LBL	23		
	23		C	13	Computes True Horiz. Dist.	st. LABELS
	11	Computes Elev. Instr.	RCL 6	34 06		A BS
	00		80 f	31		B FS
4	34 04		COS	05		C Horiz. Dist.
7	35 22		ENTER†	41		D Slope Dist.
	22		X	71		E
	01		RCL 2	34 02		0
3	34 03		X	71		1
	51		GTO	22		2
	42		0	00		3
1	34 01		LBL	23		4
	61		D	14	Computes True Slope Dist.	5
5	33 05	Elev. Instr.	90 RCL 6	34 06		6
	22		f	31		7
	00		COS	05		8
	23		RCL 2	34 02		9
	01		X	71		FLAGS
	42		GTO	22		1
3	34 03		0	00		2
	61					
1	34 01					
	61					
5	33 05		100			